ACS OMEGA

http://pubs.acs.org/journal/acsodf

Article

ZnO and TiO_2 Nanocolloids: State of Mechanisms that Regulating the Motility of the Gastrointestinal Tract and the Hepatobiliary System

Olga Tsymbalyuk, Tamara Davydovska, Vladyslav Lisnyak, Stanislav Veselsky, Alexander Zaderko, Ivan Voiteshenko, Anna Naumenko, and Valeriy Skryshevsky*

Cite This: *ACS Omega* 2021, 6, 23960−23976

Read Online

ACCESS | Metrics & More | Article Recommendations | Supporting Information

ABSTRACT: Using the transmission electron microscopy (TEM)/high-resolution TEM (HRTEM) and selected area electron diffraction (SAED) methods, it was shown that the nanocolloids of ZnO contain hydrolyzed ZnO nanoparticles (NPs). Typically, the nanocrystalline $ZnO/Zn(OH)_2$ core is covered by an amorphous shell of zinc hydroxides, preventing the encapsulated crystal core from dissolving. Similar studies were carried out with TiO_2 nanocolloids. It was found that burdening of rats for 30 days with a ZnO aqueous nanocolloid (AN) was accompanied by a narrowing of the amplitude range, a decrease (increase) in the frequency of spontaneous contractions (SCs), and an inhibition of the efficiency indices for smooth muscles (SMs) of the antrum and cecum. Under longer (100 days) burdening of rats with AN of ZnO, there was a tendency toward restoring the above parameters. In terms of the value and the direction of changes in most parameters for SCs of SMs, the effects (30 days) of TiO_2 AN differed from those for ZnO AN and were almost the same in the case of their long-term impact. It was found that mostly M2-cholinoreceptor-dependent mechanisms of regulating the intracellular concentration of Ca^{2+} were sensitive to the effect of ZnO and TiO_2 ANs. The molecular docking demonstrated that ZnO and TiO_2 NPs did not compete with acetylcholine for the site of binding to M3 and M2 cholinoreceptors but may impact the affinity of orthosteric ligands to M2 cholinoreceptors. The studies showed that burdening rats with ZnO and TiO_2 ANs was also accompanied by changes in the activity state of both intracellular enzymes and the ion transport systems for Na^+, K^+, and Ca^{2+}, related to the processes of bile secretion, via the plasma membrane of hepatocytes.

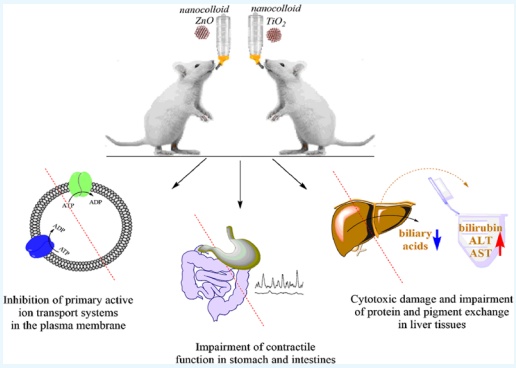

INTRODUCTION

Modern synthetic technologies are enabling the production of metal and metal oxide nanoparticles (NPs) with required physical and chemical properties.[1−3] NPs have high chemical reactivity, and, at the size of 1−2 nm, they easily react with other chemical compounds, and the activation energy for the reaction is negligibly small. As a rule, the energy accumulated by NPs is determined by uncompensated chemical bonds of the surface atoms, which are responsible for numerous superficial phenomena.[4,5] Nowadays, zinc oxide (ZnO) is one of the nanomaterials that is widely commercially available. After titanium dioxide NPs, ZnO NPs are the second most used commercial nanopowders. Bulk ZnO is a wide-band-gap semiconductor (3.37 eV).[6,7] Forming a diverse family of nanostructures, wurtzite ZnO has a layered structure that can be represented as the hexagonal closest packing of oxygen atoms, in which zinc atoms uniformly occupy half of the tetrahedral voids.[7] Because of superficial and quantum-size effects, ZnO NPs gain specific structural, electric, and optic properties, which make them an integral part and promising component of many highly technological instruments and devices.[8−10] High adsorption capacity, chemical stability, and catalytic activity of NPs as well as the ability to form free radicals on the surface[11,12] are associated with a significant specific surface area of this nanomaterial, for example, for NPs with a size of 30−50 nm, this value is 20−70 m^2/g.

ZnO NPs have a tunable surface charge, which depends on the pH of the medium. In water, ZnO NPs exhibit a positive charge at pH < 7 and neutral pH and a negative charge at pH > 7.[13] High surface area and surface charge for most ZnO NPs correlate with higher cellular uptake and greater cytotoxicity. The former and latter are required for the emergence of special biochemical properties, which are manifested even at rather low concentrations of ZnO NPs in solutions.[11,12] Currently, for

Received: June 7, 2021
Accepted: August 20, 2021
Published: September 9, 2021

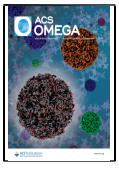

substantiating the mechanisms of their antibacterial action, the structural and energetic parameters of ZnO NPs are intensively studied with quantum-chemical calculations. The production of reactive oxygen species (ROS) on the surface and the partial dissolution of ZnO NPs with the release of cytotoxic Zn^{2+} ions destructed the integrity of cells that are accompanied by a decrease in the metabolism of amino acids and violation of the enzyme system.[11−14] Because of this, ZnO NPs are used in modern pharmacology as antimicrobial preservatives. According to the data of the U.S. Food and Drug Administration (21CFR 182.8991), zinc oxide is also used as a food additive.[14,15] With long-term intake of ZnO nanomaterials, there is an unanswered question about the motility of the gastrointestinal tract (GIT), whose abnormal processes of regulating excitation−inhibition[16,17] may cause its impaired functioning, for instance, the changes in intestinal pressure, and thus in the filtration of solutions, aqueous nanocolloids, from the gastric cavity and intestines to blood and lymph and in the movement of chyme residues. There is a pharmacological aspect of the problem related to one of the relevant links in regulating GIT motility—the states of M3 and M2 cholinoreception under these conditions—an important targeted component of most drugs. It is noteworthy that the problem of toxic activity of nanocolloids on digestion processes in GIT may be expanded by another, still not investigated, issue regarding the condition of metabolism processes in hepatocytes. The hepatocytes are potential targets for nanocolloids, which enter the systemic blood flow via the portal vein after being adsorbed within a GIT wall and then come to the liver. As the research of the abovementioned issues is important, they became the subject of our studies. To ensure a deeper understanding of the specificities in the structural organization of nanomaterials in the impact of their nanocolloids on biological processes, the results of experiments are presented in the paper as a comparison of the changes in the parameters under investigation at the effect of nanocolloids of ZnO and TiO_2 (with nanoparticles of almost the same or close size).

RESULTS AND DISCUSSION

X-ray powder diffraction (XRPD) patterns of TiO_2 and ZnO NPs are shown in Figures S1 and S2, respectively. In Figure S1, the XRPD pattern of TiO_2 NPs exhibited strong diffraction peaks at 25.3, 37.7, and 48°, indicating an anatase TiO_2 structure (Sp. gr. $I4_1/amd$, a = 3.796, c = 9.529 Å). On the other hand, this XRPD pattern exhibited strong diffraction peaks of lower intensities at 27.2, 36, and 54.8°, indicating a TiO_2 rutile phase ($P4_2/mnm$, a = 4.61 Å, c = 2.96 Å) as a minor component. All diffraction peaks are in good agreement with the standard JCPDS no. 88-1175 and 84-1286 patterns. These results suggested that the powder of TiO_2 is composed of anatase and rutile crystallites. The XRPD pattern of the ZnO NPs is shown in Figure S2. All observed diffraction peaks can be indexed to the ZnO wurtzite structure (JCPDS card number 36-1451); the lattice parameters of the prepared ZnO NPs were obtained: a = 3.22 Å, c = 5.20 Å. The peak positions observed at about 15.45, 26.0, 27.5, and 30.52° for this sample resemble those of the β-$Zn(OH)_2$ crystal structure (JCPDS card number 20-1435). X-ray amorphous components contribute to the broadening of the XRPD patterns; however, this effect is negligible.

Transmission electron microscopy (TEM)/high-resolution TEM (HRTEM) images show morphologic features of ZnO NPs (Figure 1a−c). Their size varies in the range from 15 to 70 nm, and plenty of them have an average size of about 25 nm

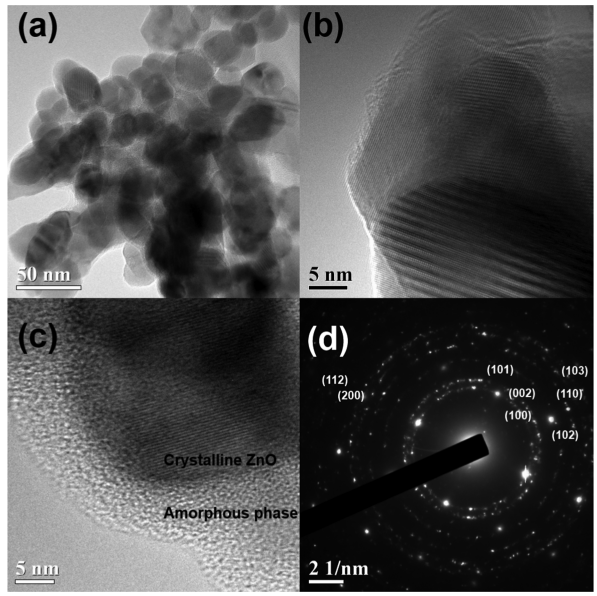

Figure 1. (a) TEM and (b, c) HRTEM images, and (d) SAED pattern of the pristine ZnO NPs.

(Figure 1a). Besides, their grains have a pronounced crystallinity, but it also presented an amorphous phase in the NPs (Figure 1b,c). Selected area electron diffraction (SAED) patterns are of high intensity and match the Miller indices of wurtzite (hexagonal) ZnO (see respective planes in Figure 1d). In addition, many other spots clearly seen in Figure 1d could be assigned to β-$Zn(OH)_2$.

The bright-field TEM image of ZnO NPs (Figure 1b) shows randomly oriented NPs with clear diffraction fringes. This feature, being visible at large nanostructured sites, confirms the highest crystallinity of ZnO/β-$Zn(OH)_2$ cores. HRTEM images show several ultrathin ZnO NPs closely placed to each other (Figure 1b,c). From these figures, one can see the fringes with a lattice spacing of about 0.3 nm. They correspond to the (002) plane of wurtzite ZnO.

After soaking in water, the average size of ZnO NPs showed a decrease when compared with that of the pristine ZnO NPs (Figure 2a−c). Because of hydrolysis of ZnO (ZnO + H_2O → $Zn(OH)_2$) and amorphization of β-$Zn(OH)_2$, here we obtained typical core−shell structures, where a thin zinc hydroxide shell, which is X-ray amorphous, covers the surface of the crystalline ZnO/β-$Zn(OH)_2$ core. The formation of such zinc hydroxide shells has lowered the crystallinity of ZnO NPs since the shell has a pronounced amorphous character (Figure 2a−c). This semiamorphous character was confirmed by SAED, as seen by the ring and spot patterns (Figure 2d). Figure 2c shows the bright-field TEM image in which is seen the hydrolyzed ZnO NPs. In the image, the crystalline phase is shown by the fringe patterns. The SAED showed less intense diffraction images, as compared with that in Figure 1d. In typical SAED patterns, there are broad rings typical for semiamorphous solids. Diffraction rings of wurtzite ZnO, which are labeled as (100), (101), and (110) and assigned to respective wurtzite planes, and some diffraction spots corresponding to (112) and (103) planes confirmed the presence of crystalline wurtzite cores.

https://doi.org/10.1021/acsomega.1c02981
ACS Omega 2021, 6, 23960−23976

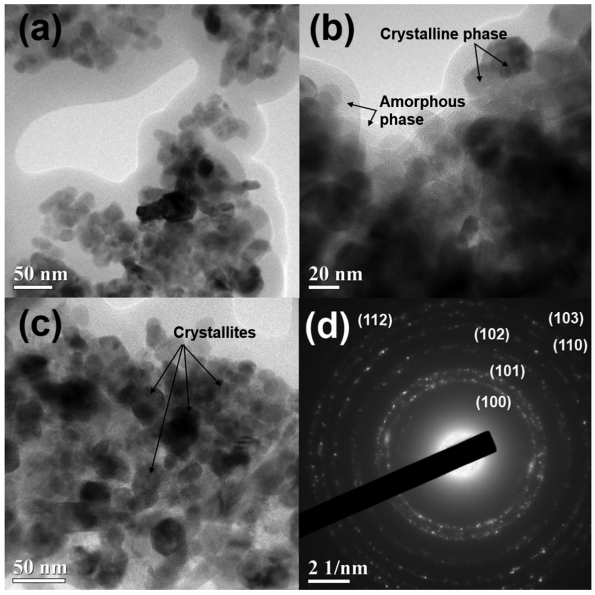

Figure 2. (a–c) TEM images and (d) SAED pattern of ZnO NPs after hydrolysis.

As expected, the hydrophilicity of the shell prevents the encapsulated crystalline ZnO/β-Zn(OH)$_2$ core from dissolution in water. TEM observations confirmed the fact that we operated with a colloidal solution of zinc hydroxide/zinc oxide core–shell NPs, hereafter referred to as ZnO nanocolloids (Figure 2c). Such ZnO nanocolloids differ from the water solutions of zinc ions, zinc complexes, or zinc hydroxide, and so this difference can be a reason for physiological effects observed at the per-oral feeding of rats.

If one considers TiO_2 NPs, Figure 3a–d shows TEM images and Figure 3e,f presents the SAED patterns of the pristine TiO_2 NPs; their primary size is 25 ± 5 nm and is close to that of ZnO NPs (cf. Figures 3a and 1a). The TEM image in Figure 3b shows that the outer hydrolyzed semiamorphous titania (HT) shell covers the TiO_2 core. Typically, the completely covering and semipermeable shell structure prevents "access" of different molecules to and from the TiO_2 core. The studied TiO_2 NPs have a rectangular shape; the size of the TiO_2 core is well-preserved in water nanocolloids. However, most particles appear as aggregates observed in the TEM micrographs presented in Figure 3a–d.

The SAED images demonstrate that bright spots appear everywhere in diffraction images (Figure 3e,f). According to electron diffraction data, two distinct crystalline phases are present in the structure of HT/TiO_2 NPs. According to the SAED images, these two kinds of phases are well crystallized. It was found, from the diffraction analysis, Figure 3e,f shows (101)a and (101)r diffraction spots assigned to anatase and rutile phases, respectively. In the TEM lattice fringes, the interplanar distances are in the range of 0.354–0.347 and 0.252–0.257 nm. They are assigned to the (101) planes of the anatase and rutile TiO_2 nanocrystals, respectively.

Hydroxylation, as any surface modification, aims at protection of TiO_2 NPs in media of different acidities. Figure 4a–f shows the core–shell TiO_2 nanostructures with crystalline anatase and rutile cores and the HT shell in the HT/TiO_2 NPs in their water nanocolloids. The HT core prevents dissolution and amorphization of the anatase and rutile cores. As shown in Figure 4a,b, after dispersing in water,

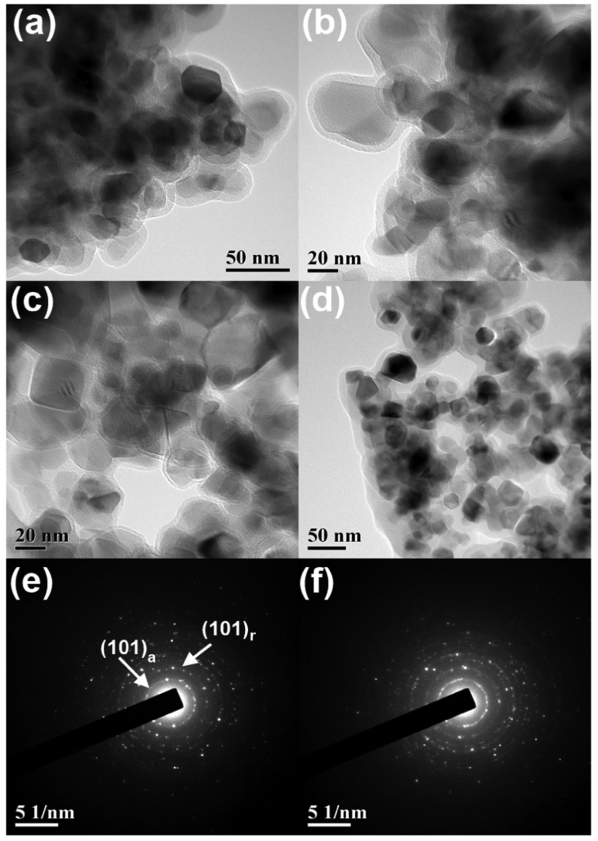

Figure 3. (a–d) TEM images and (e, f) SAED patterns of the pristine HT/TiO_2 NPs.

the average size of the individual HT/TiO_2 NPs is about 15 ± 5 nm. The shell thickness of semiamorphous HT is estimated to be in the range from 2.5 ± 0.5 to 5.0 ± 0.5 nm (Figure 4c,d,f; Figures S3a and 3b). According to SAED images (Figure S3c,d), there are no observable changes in crystallinity for the anatase and rutile phases presented in the water nanocolloids.

Study of the Condition of Spontaneous Contractile Activity of SMs of Gastric Antrum and Cecum of Rats Burdened with ZnO and TiO_2 ANs (Compared Using the Data[18,19] of the Authors). As stated above, the physical–chemical properties of ZnO ANs are notable for pH-dependent changes in the charge of the surface of NPs. At the same time, the material acquires new physical–chemical properties that must be crucial for the manifestation of its cytotoxicity.[13,20]

Comparison. Both ZnO and TiO_2 NPs are hydrolysable in an aqueous electrolyte solution, forming a stable aqueous nanocolloid with different amphoteric forms of hydroxides: Ti(OH)$_4$, TiO(OH)$_2$, $TiO_2 \cdot 2H_2O$, H_4TiO_4, H_2TiO_3, and $TiO_2 \cdot H_2O$; the prevalence of each of them in the nanocolloid is pH-dependent. It also impacts their surface-specific properties and cytotoxicities.[21−23] Therefore, in our study, we investigated smooth muscles of the gastric antrum and cecum of rats, whose pH values of media are different, namely, the antrum: 3.2 for feeding, 3.9 for fasting, and 6.6 was the average value for the intestines.[24] In our work, the tenzometric method in the isometric mode was used to investigate the spontaneous contractile activity of the isolated circular SM stripes of the antrum and cecum of three groups of rats: the control group (n = 6) and two groups of animals (six in each) burdened with ZnO AN for 30 and 100 days. It is known[25−28]

https://doi.org/10.1021/acsomega.1c02981
ACS Omega 2021, 6, 23960−23976

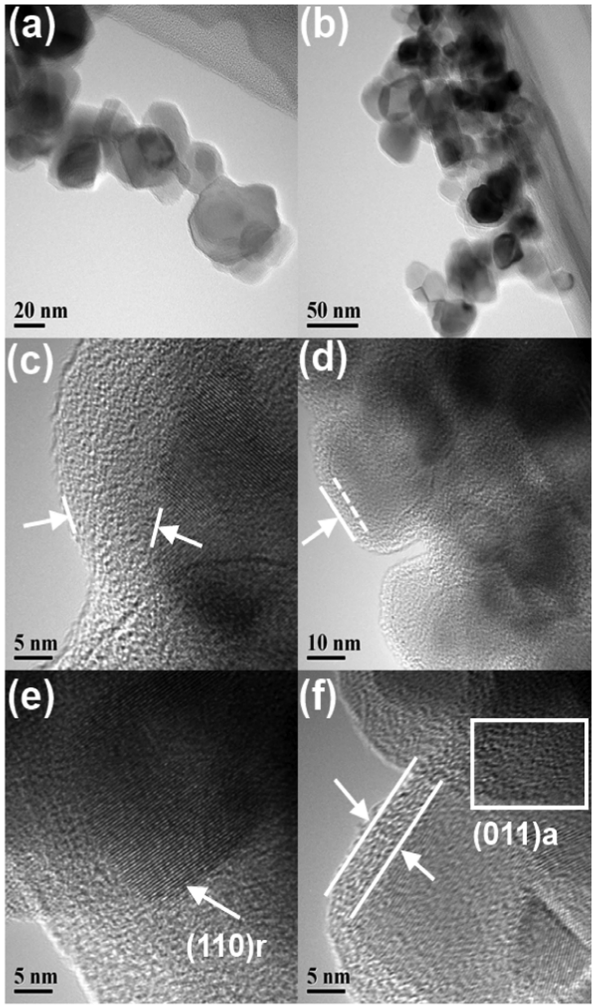

Figure 4. (a, b) TEM and (c–f) HRTEM images. Core–shell TiO_2 nanostructures with crystalline anatase and rutile cores and hydroxylated shell in the HT/TiO_2 NPs in ANs.

that the generation and regulation of spontaneous electric activity of SMs in GIT, and thus its motility, occur with the involvement of interstitial cells of Cajal (ICC)—components of the heterogeneous population of cells from its wall (neurons, SMC, immune cells)—and is controlled by enteric and vegetative nervous systems, but even in the absence of the impact of neuromediators and hormones, spontaneous action potentials and thus SM contractions are registered. ICC populations of the antrum and cecum are represented by similar subtypes of these cells, but these populations differ by the presence of interstitial cells with different amplitude–frequency parameters of pacemaker currents, namely, ICC–DMP and ICC–SMY.[29]

Our studies demonstrated that the differences in the mechanisms of regulating spontaneous contractions in SMs of the murine antrum and cecum in the control group (60 min of registration) were manifested in quantitative values of the frequency of their contractions for 10 min, the magnitude of which in the SMs of the cecum (Figures 5a and 6(1)) exceeded the same parameter for SMs of the antrum three times (Figures 7a and 8(1)). The averaged values for the duration of spontaneous contraction–relaxation cycles in these objects also differed by several orders.

In the smooth muscles of the cecum (Figure 6(2)), this process occurred much faster than in SMs of the antrum (Figure 8(2)). A relevant parameter, characterizing the coordination between energy-independent and energy-dependent processes of regulating intracellular concentration of Ca^{2+} ions in SMC of GIT, is the asymmetry coefficient, whose values in the cycles of spontaneous contractions–relaxations in SMs of the cecum exceeded the same parameter for the antrum by 1.5 times, while the indices of their working efficiency—AU indices—had an almost threefold difference. The mentioned index had higher values in SMs of the antrum (Figures 6(3) and 8(3)). As for the range of amplitudes within which spontaneous contractions occurred in SMs of the antrum and cecum, they did not have relevant differences, amounting to 2–18 and 1–12.5 mN, respectively; n = 12. The study on the spontaneous contractile activity of SMs of the cecum and antrum of two groups of rats burdened for 30 days with ZnO ANs in the abovementioned concentration demonstrated that, as compared with the control (Figures 5a and 7a), there was 7-fold (Figure 5b) and 12-fold (Figure 12b) narrowing in the amplitude range for spontaneous contractions; n = 12. Under the same conditions of experiments, the changes in spontaneous contractions in 10 min were different in their directions with regard to the control—SMs of the cecum and antrum, respectively, had a twofold decrease (Figure 6(1)) and a threefold increase (Figure 8(1)) in the first and second cases; n = 12. Therefore, the duration of contractions–relaxations in SMs of the cecum increased twice (Figure 6(2)), while in SMs of the antrum, this parameter decreased almost three times (Figure 8(2)); n = 12. Noteworthy are the changes in the frequency characteristics of spontaneous contractions of SMs of the cecum and antrum because of the effect of the ZnO nanocolloid under these conditions; thus, as stated above, these are extremely important changes in intraintestinal and intragastric pressure, the modulation of which will impact the filtration of solutions to the blood and lymph.

In our experiments, the asymmetry coefficients, in SMs of both the cecum and antrum, were within the control. At the same time, as compared with the control group, the indices of efficient functioning for SMs of the cecum and antrum—AU indices—decreased considerably: 3.2 times and almost 14 times, respectively (n = 12). Although the AU indices of the cecum and antrum in the control group differed more than threefold, because of the effect of ZnO NPs, they decreased considerably and reached almost identical values (Figures 6(3) and 8(3)). As stated above, when the rats were burdened with ZnO AN, the frequency of the spontaneous contractions of SMs in the cecum and antrum had different changes in terms of directions of their effects and values, which, considering the experimental data reported in refs26, 29, may be assumed to be the result of the impact of AN on ICC, differing in these areas by their amplitude–frequency characteristics of pacemaker activity, the formation of which is known[28] to occur with the involvement of nonselective cation TRPC4 channels, also related to inositol-1,4,5-triphosphate (IP3)-induced release of Ca^{2+} ions from the IP3-sensitive depot of the sarcoplasmic reticulum (SR) with their subsequent intake in mitochondria, to maintain the oscillation of the intracellular concentration of these cations. The carcasses holding the abovementioned proteins are caveolin proteins—the constituents of caveolae, through which ions, molecules of organic substances, and NPs may penetrate similar to SMCs of GIT.[30,31] The frequency of fluctuations in the concentration of Ca^{2+} cations is on the same

https://doi.org/10.1021/acsomega.1c02981
ACS Omega 2021, 6, 23960–23976

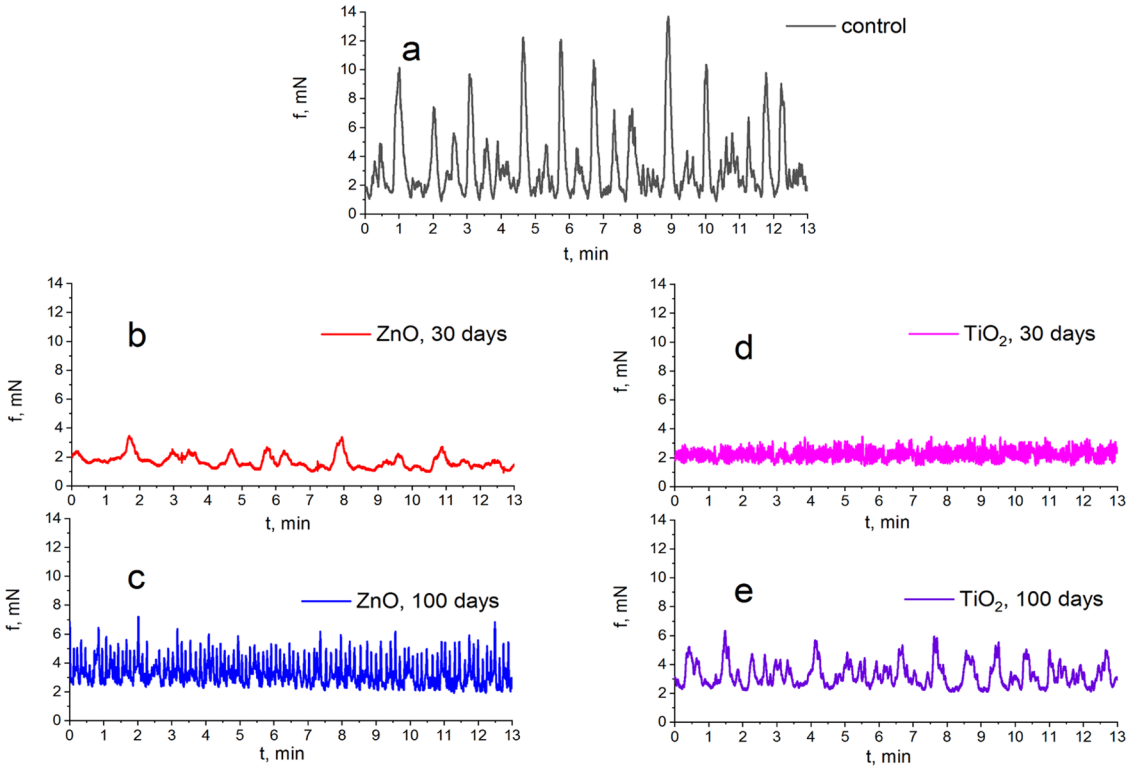

Figure 5. Spontaneous contractile activity of the circular SMs of the cecum of rats: (a) control group and groups of rats burdened with ZnO ANs for (b) 30 days and (c) 100 days and with TiO_2 ANs for (d) 30 days and (e) 100 days.

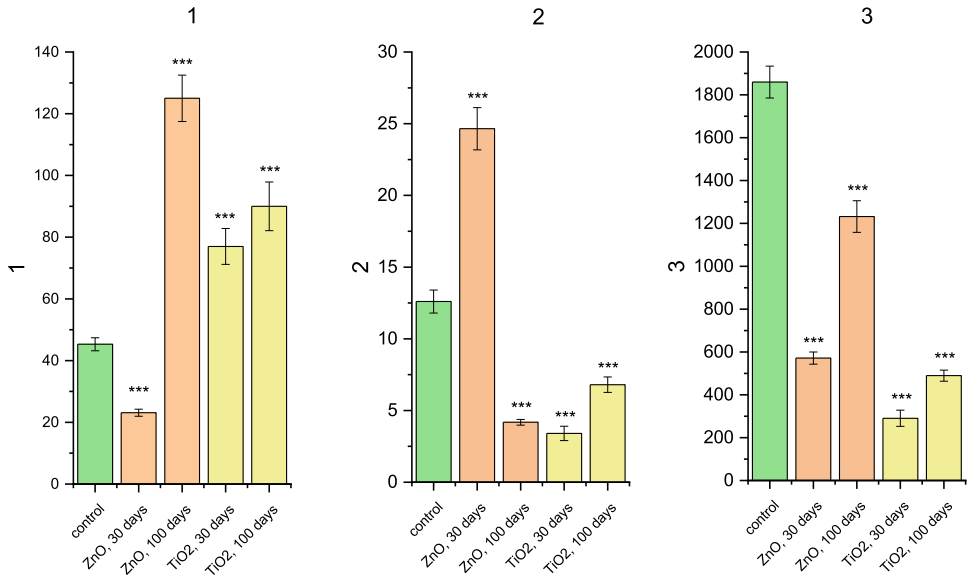

Figure 6. Histograms of the kinetic parameters for the spontaneous contractile activity of the circular SMs of the cecum (control; 30 and 100 days of burdening the rats with ZnO ANs; 30 and 100 days of burdening the rats with TiO_2 ANs, $n = 6$). 1, frequency of preparation contractions for 10 min; 2, averaged value of the duration of the contraction−relaxation cycle; 3, AU index of contractions; ***$p < 0.001$ indicates reliability of changes as compared with the control.

order as the pacemaker currents of ICC. It should be noted that caveolin-1 and caveolin-2 are known[30] to be highly expressed in the caveolae of ICC-SM, which are the components of the ICC population of the cecum SMs (located on the submucous surface of the circular muscle layer), but are absent from the antrum SMs.

Comparison of Changes in Parameters: AU indices, the ranges of amplitudes, the ranges of spontaneous contractions in SMs of the cecum and antrum of rats burdened with ZnO and TiO_2 ANs for 30 days (the size of NPs 21 ± 5 nm); the concentration of 0.1 mg/kg of bodyweight in 24 h (the average daily intake of a food additive E171 into a human organism in Great Britain).[18]

SMs of the Cecum. Changes in parameters by direction: AU indices and the amplitude range coincided, but the frequencies of contractions did not coincide (Figure 6(3), Figure 6(1), and

https://doi.org/10.1021/acsomega.1c02981
ACS Omega 2021, 6, 23960−23976

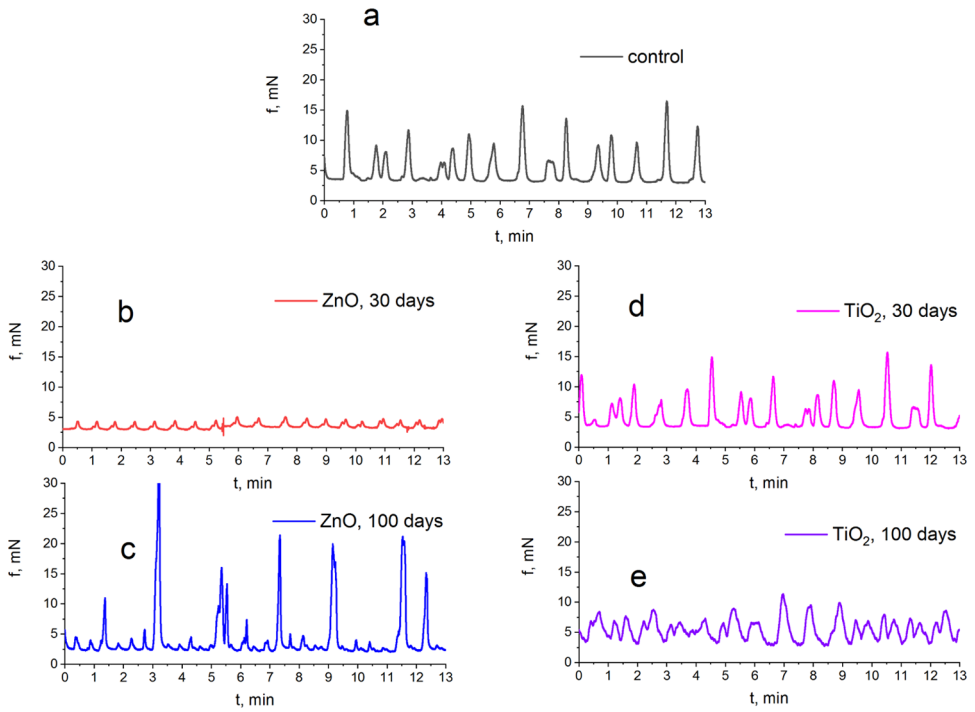

Figure 7. Spontaneous contractile activity of the circular SMs of the murine antrum: (a) control group and groups of rats burdened with ZnO ANs for (b) 30 days and (c) 100 days and with TiO_2 ANs for (d) 30 days and (e) 100 days.

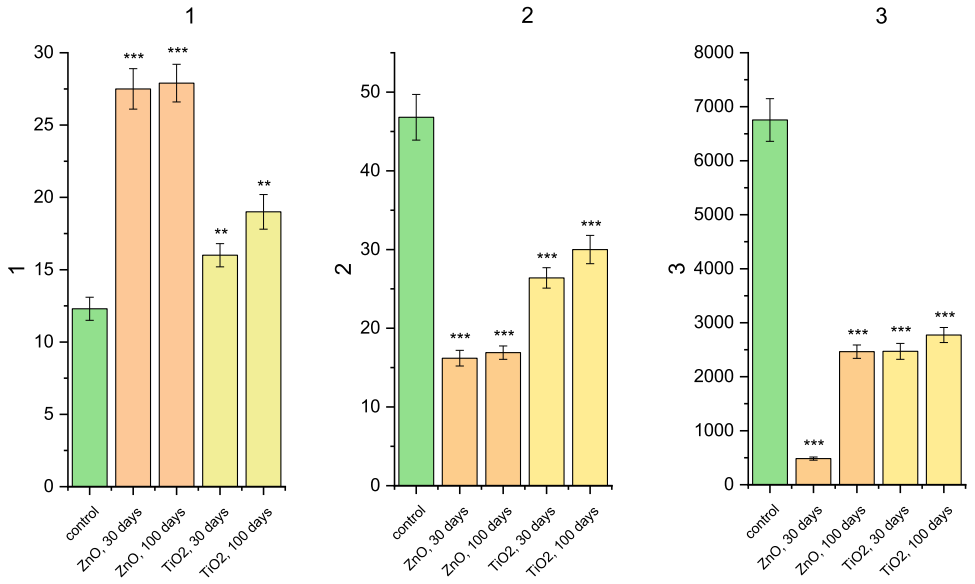

Figure 8. Histograms of the kinetic parameters for the spontaneous contractile activity of the circular SMs of the antrum (control; 30 and 100 days of burdening the rats with aqueous ZnO nanocolloids; 30 and 100 days of burdening the rats with TiO_2 ANs; $n = 6$). 1, frequency of preparation contractions for 10 min; 2, averaged value of the duration of the contraction−relaxation cycle; 3, AU index of contractions; ***$p < 0.001$ indicates reliability of changes as compared with the control.

Figure 9). Changes in parameters by value: The most considerable changes were registered in the ranges of amplitudes of spontaneous contractions when rats were burdened with ZnO and TiO_2 ANs, as well in AU indices when burdening rats with TiO_2 AN (Figures 6(3) and 9).

SMs of the Antrum. Changes in parameters by direction: all parameters coincided (Figures 8(1), 8(3), 9). Changes in parameters by value: There were critical changes in the AU indices and amplitude ranges when rats were burdened with ZnO ANs (Figures 8(3) and 9). Thus, ZnO and TiO_2 ANs modulated the mechanisms of regulating the spontaneous contractile activity of both SMs of the cecum and antrum of rats burdened with these nanomaterials for 30 days. The activity of these nanomaterials did not coincide when comparing all results of their impact on the formation of frequency characteristics of spontaneous contractions in cecum SMs. On the contrary, in the antrum SMs, these changes were unidirectional and caused hyperstimulation of this parameter. At the same time, there was an absolute coincidence in the direction but considerable differences in the values of changes

https://doi.org/10.1021/acsomega.1c02981
ACS Omega 2021, 6, 23960−23976

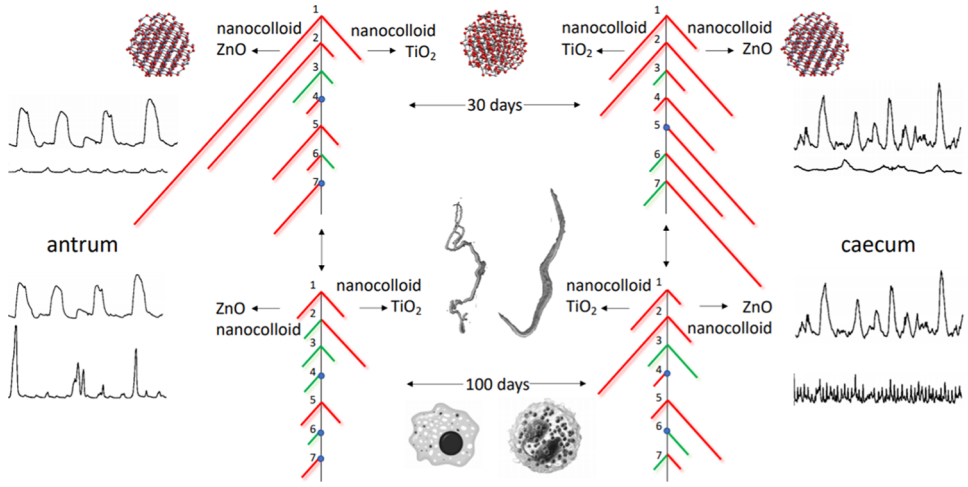

Figure 9. Scheme comparing the changes in the parameters of spontaneous contractile activity and SM contractions in the antrum and cecum, induced by HKS and acetylcholine in rats, burdened by ZnO and TiO_2 ANs for 30 and 100 days. 1, 2, and 3 represent, respectively, changes in the efficiency coefficients for the SM function, the amplitude range, and the frequency of spontaneous SM contractions; 4 and 5 represent, respectively, changes in the phase and tonic components of high-potassium contracture of SMs; and 6 and 7 represent, respectively, changes in the phase and tonic components of acetylcholine-induced SM contractions. The inhibition and enhancement of the abovementioned parameters, as compared with the control, are highlighted in red and green, respectively.

in the range of amplitudes of spontaneous contractions, the AU indices of both the cecum and antrum when the rats were burdened with ZnO and TiO_2 ANs.

The analysis of our results for changes in the parameters of spontaneous contractions of SMs of the cecum and antrum of rats burdened with the ZnO AN in the abovementioned concentration for 100 days and their comparison with the results of measurements of similar parameters in rats burdened with this nanomaterial for 30 days demonstrated the tendencies toward the restoration of AU indices and the amplitude range to the control level. As stated above, when rats were burdened with ZnO NPs for 30 days, the range of amplitudes of spontaneous contractions of the antrum SM, as compared with the control, decreased 12 times; n = 12. However, in 100 days, these changes were much smaller (1.8 times; n = 12) and opposite in their direction (toward hyperstimulation). The AU indices on the 30th day of burdening rats with this nanomaterial (if compared with the control) decreased 14 times (n = 12), whereas on the 100th day, it was 2.6 times (n = 12) (cf. Figures 6(3) and 8(3)). The asymmetry coefficients in the first and second cases remained within the control. Similar tendencies were observed regarding the changes in the abovementioned parameters of spontaneous contractile activity, in this case, the cecum SMs (Figures 5 and 6). According to the scientific data obtained on the immune system model, while overcoming the barrier of the digestive tract wall, ZnO NPs may be captured by immune-competent cells and be subject to removal from the organism with time. However, in the initial stages, the aforementioned process leads to different toxic reactions accompanied by a decrease in their viability, formation of ROS, apoptosis, etc. Here, the result of the decrease in NPs in the organism will also be determined by the factor of time required to restore the functions of the very immune system after contact with the nanomaterial.

Comparison of Changes in Parameters: AU Indices, Ranges of Amplitudes, and Frequencies of Spontaneous Contractions of SMs of the Cecum and Antrum of Rats Burdened for 100 days with Aqueous Nanocolloids of ZnO and TiO_2. *SMs of the Cecum.* Changes in parameters by direction: All parameters coincided. Changes in parameters by value: The most considerable changes were registered in the ranges of amplitudes when burdening rats with TiO_2 ANs.

SMs of the Antrum. Changes in parameters by direction: AU indices and contraction frequencies coincided, but the ranges of amplitudes did not coincide. Changes in parameters by value: The most considerable changes were registered in the amplitude ranges of spontaneous contractions when burdening rats with TiO_2 ANs (Figures 7, 8, and 9). Therefore, when rats were burdened with ZnO AN for 100 days, there was a decrease in the value and a change in the direction of its impact on the spontaneous activity of SMs of the murine cecum and antrum. There was a prevalence of hyperstimulation effects, which were values of the same order. The effects of TiO_2 ANs on SMs of the cecum and antrum differed in the direction of changes in parameters of spontaneous contractions in most cases.

Study of the Condition of Contractions, Induced by High-Potassium Krebs Solution and Acetylcholine, in SMs of the Antrum and Cecum of Rats Burdened with ZnO and TiO_2 ANs (According to Previous Data[28,29]). Considering the abovementioned results of the studies, it was interesting to determine the involvement of both mechanisms of regulating the pacemaker activity of ICC and the mechanisms of potential-dependent regulation of Ca^{2+} in SMS on the effects of nanocolloids on the spontaneous contractile activity of SMs of the cecum and antrum. Therefore, the next series of experiments was aimed at investigating the contracture state of SMs of the murine cecum and antrum, induced by a high-potassium Krebs solution (HKS) (80 mM), whose phase component is known to be based[32,33] on the depolarization of the membrane and potential-dependent input of extracellular Ca^{2+} ions to SMC through voltage-gated Ca^{2+} channels (VGCs) of L-type with the subsequent release of Ca^{2+} ions from the sarcoplasmic reticulum. In the experiment, the muscle preparations of the cecum and antrum from the control group of rats developed

https://doi.org/10.1021/acsomega.1c02981
ACS Omega 2021, 6, 23960−23976

contractions−relaxations in response to the application of SMC, the average values of the phase component of which were 19 ± 1.4 mN at n = 12 and 23 ± 1.3 mN at n = 12; the ratio between the phase component and the tonic component in both kinds of muscles was almost the same: (1.04 ± 0.1) at n = 12 and (1.2 ± 0.08) at n = 12, respectively. When rats were burdened for 30 days with ZnO AN in the abovementioned concentration, there was a 5-fold decrease (n = 12) in the phase component and a 9.5-fold decrease (n = 12) in the tonic component of HKS in SMs of the cecum as compared with the control. Under long-term burdening (for 100 days), the phase component of HKS of cecum SMs was at the level of the control, whereas the tonic component decreased 5.4 times instead of 9.5 times (n = 12). As for antrum SMs, when burdening rats with this nanomaterial for 30 days, the changes in the HKS parameters were much smaller as compared with the cecum SMs: the phase component decreased by (27.4 ± 1.8) % (n = 12), $p < 0.05$ as compared with the control, while the tonic component was 5.5 times smaller than the control (n = 12). When rats were burdened with ZnO AN for 100 days, there was a 1.8-fold increase (n = 12) in the phase component of HKS and a 2.2-fold decrease in the tonic component as compared with the control. The study on SM contractions in the cecum and antrum, induced by the application of caffeine (20 mM) in nominally calcium-free Krebs solution to rats burdened with ZnO AN for 30 and 100 days, showed that their amplitudes remained within the control, which demonstrated no changes in the mechanisms of the release of these cations from the sarcoplasmic reticulum of these muscles SMCs.

Comparison of Changes in Parameters: Phase and Tonic Components of HKS of SMs of the Cecum and Antrum of Rats Burdened with Nanocolloids of ZnO and TiO_2. *SMs of the Cecum.* The duration of burdening was 30 days. Changes in parameters by direction: No coincidence was found in the parameters. Changes in parameters by value: The most considerable changes were registered in the tonic component of HKS when burdening rats with ZnO AN. The duration of burdening was 100 days. Changes in parameters by direction: No coincidence was found in the phase components. Changes in parameters by value: The most considerable changes were registered in the tonic component of HKS when burdening rats with ZnO AN.

SMs of the Antrum. The duration of burdening was 30 days. Changes in parameters by direction: Tonic components coincided. Changes in parameters by value: The most considerable changes were registered in the tonic component of HKS when burdening rats with ZnO AN. The duration of burdening was 100 days. Changes in parameters by direction: Tonic components coincided. Changes in parameters by value: The changes in tonic components of HKS when burdening rats with ZnO and TiO_2 ANs were of the same values (Figure 9). Thus, the abovementioned results of the studies demonstrated that regardless of the duration of burdening rats with aqueous nanocolloids of ZnO and TiO_2, the unidirectional changes occurred mostly in the tonic component of high-potassium contracture of SMs of the cecum and antrum, the relevant role in the formation of which is known[33] to belong to the mechanisms of controlling the intracellular concentration of Ca^{2+} during potential-dependent intake of these cations into SMC through VGC of L-type and the mechanisms of the release of mediators from nerve endings of the intramural nervous system.

It is known from the scientific literature[16,17,34] that the parasympathetic control of the contractile activity of all of the visceral and some vascular smooth muscles takes place with the involvement of acetylcholine (AC), the main excitation neurotransmitter. Taking this fact into consideration, the next series of experiments was aimed at investigating the acetylcholine-induced (concentration of 10^{-5} mol/L) contractions of SMs of the cecum and antrum of rats burdened with an aqueous nanocolloid of ZnO for 30 and 100 days. In the control, the averaged value of the phase component of contractions in the cecum SMs, induced by this agonist in the abovementioned concentration, was (15 ± 0.9) mN (n = 12), which was almost twice smaller than in the antrum SMs (26.3 ± 1.8) mN (n = 12), while its ratio with the tonic component was the same for both kinds of muscles: (1.5 ± 0.1), n = 12 and (1.3 ± 0.08), n = 12, respectively. The studies demonstrated that as compared with the control group of rats, the ones burdened with an aqueous ZnO nanocolloid for 30 days had the inhibition of the phase component of SM contraction, induced by acetylcholine with much greater changes in this parameter for cecum SMs (6 times, n = 12) than for antrum SMs (1.64 times, n = 12).

Zholos et al.[34] postulated that the formation of the phase component of AC-induced contraction of GIT smooth muscles is related to the activation of the signaling cascade: muscarinic choline type 3 receptor−G_q/G_{11} proteins−phospholipase C_β− resulting in the generation of inositol-1,4,5-triphosphate (IP_3), induced by the release of Ca^{2+} from the IP_3-sensitive depot of SR. The activation of muscarinic choline M3-type receptors by acetylcholine is also accompanied by the depolarization of the plasmatic membrane, the activation of VGC of L-type, and the intake of extracellular ions Ca^{2+} to SMC with subsequent Ca^{2+}-induced release of Ca^{2+} from the ryanodine-sensitive depot of SR and SM contraction. Taking the abovementioned factors into consideration, one may assume that under these conditions the decrease in the phase component of AC-induced contraction of SMs of the cecum and antrum could have been caused by the inhibition of the mechanisms of Ca^{2+} ions input to SMC and the release of these cations from SR; however, the results of the experiments demonstrated that the contractions of SMs of both the cecum and antrum, induced by acetylcholine in nominally calcium-free Krebs solution (10^{-5} mol/L), remained within the control. Considering also[35] that the initial acetylcholine-induced increase $[Ca_i^{2+}]$ declines soon, and the activity of the kinase of myosin light chains reaches a high level, it is also probable that the reason for the inhibited phase component of AC-induced contraction when burdening rats with ZnO AN is also a decrease in the sensitivity of the contractile apparatus of SMC to Ca^{2+} ions.

The experiments demonstrated that both SMs of the cecum and antrum had a considerable 10-fold decrease in the value of the tonic component of AC-induced contraction compared to the control (n = 12) and a 5-fold decrease (n = 12), which, considering the mechanism of its formation,[17,34,35] may be caused by the ZnO AN during the cholinergic excitation of the change in M2 receptor-dependent mechanisms, limiting the input of extracellular Ca^{2+} ions into SM cells via VGC of L-type. The burdening of rats with ZnO AN for 100 days was accompanied not by the inhibition but by the increase in SMs of the cecum and antrum as compared with the control—2.5-fold (n = 12)—and by (36 ± 2.3) % (n = 12), $p < 0.05$, in the phase component of AC-induced contractions, while tonic components decreased twice (n = 12).

https://doi.org/10.1021/acsomega.1c02981
ACS Omega 2021, 6, 23960−23976

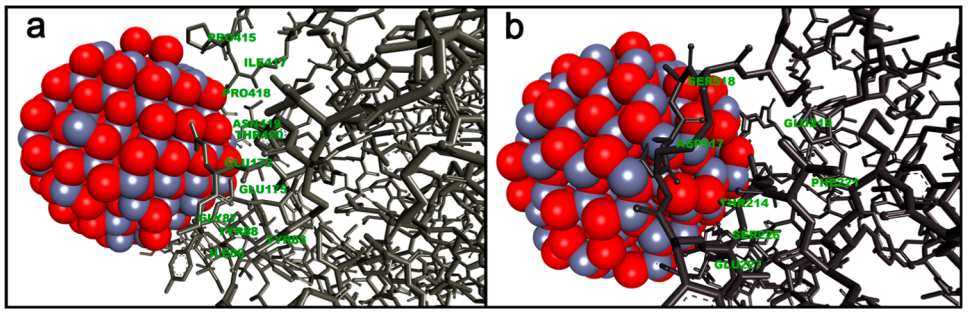

Figure 10. (a) Site of ZnO NP binding to the M2 muscarinic receptor; (b) site of ZnO NP binding to the M3 muscarinic receptor.

Comparison of Changes in Parameters: Phase and Tonic Components and AC-Induced Contractions in SMs of the Cecum and Antrum of Rats Burdened with ZnO and TiO_2 ANs. *SMs of the Cecum.* The duration of burdening was 30 days. Changes in parameters by direction: All parameters did not coincide. Changes in parameters by value: The most considerable changes were registered in the tonic component of SM when burdening rats with ZnO AN. The duration of burdening was 100 days. Changes in parameters by direction: All parameters did not coincide. Changes in parameters by value: All parameters acquired almost similar values.

SMs of the Antrum. The duration of burdening was 30 days. Changes in parameters by direction: All parameters did not coincide. Changes in parameters by value: The most considerable changes were registered in the tonic component of AC-induced SM contractions when burdening rats with ZnO AN. The duration of burdening was 100 days. Changes in parameters by direction: All parameters did not coincide. Changes in parameters by value: When burdening rats with an aqueous nanocolloid of TiO_2 NPs, all parameters were within the control range, while when burdening rats with an aqueous nanocolloid of ZnO NPs, there was an increase in the phase component and a decrease in the tonic component of AC-induced contractions (Figure 9). Therefore, our results demonstrated that the 30 day long burdening of rats with ZnO AN was accompanied by a considerable inhibition of M3 and M2 receptor-dependent mechanisms of regulation $[Ca_i^{2+}]$ in the cecum and antrum during the cholinergic excitation with more significant changes in the M2 receptor-dependent mechanism. Under these conditions, the effects of the TiO_2 AN were opposite in their directions and much smaller in their scope. It may be assumed that the reasons for the changes in cholinergic excitation of SMs may be the formation of the sites of binding ZnO NPs and TiO_2 NPs by muscarinic choline M3- and M2-type receptors jointly with acetylcholine, which became the subject of our further studies. The restoration to the control level for phase and tonic components of AC-induced contractions of the cecum SMs (except for the tonic component) and the antrum SMs when burdening rats with an aqueous nanocolloid of TiO_2 and a considerable decrease in these parameters when burdening rats with an aqueous nanocolloid of ZnO took place during longer burdening (100 days) of rats with these nanomaterials (Figure 9).

Molecular Docking of Nanostructured ZnO and TiO_2 with Muscarinic Choline M2- and M3-Type Receptors. Spherical ZnO and TiO_2 NPs of 5 nm were simulated to identify the set of typical bonds: crystalline structure of the nanoparticle—choline receptor. First, the selected form of the nanoparticles ensured comprehensive investigation of coordination bonds of docking properly, and second, it allowed for less complicated and time-consuming calculations. Similar interfaces of the interaction with choline receptors may be expected for larger NPs, albeit in a higher amount. The requirements to the time of calculations and resources would increase by several orders. The molecular docking of a spherical ZnO NP with a muscarinic choline M2-type receptor demonstrated that the binding site and its environment included 11 amino acid residues (Figure 10a), among which the ratio of polar uncharged, nonpolar, and polar charged amino acid residues was 0.36:0.45:0.18, with the respective distribution of the Gibbs free energy (kJ/mol) being (−0.52), (5.54), and (−0.54). Geometric shape complementarity score (Score), approximate interface area (Area), and atomic contact energy (ACE) calculated on the PatchDock webserver have the following values: 4140, 625.40 $Å^2$, and 20.53 kJ/mol, respectively. The binding site and its environment of the spherical TiO_2 NP with this receptor had 10 amino acid residues (Figure 10b), with the ratio in terms of polarity being 0.3:0.5:0.2, and the distribution of the Gibbs free energy (kJ/mol) was (−0.35), (5), and (−0.54). The comparative analysis of the binding sites for TiO_2 and ZnO NPs with the muscarinic M2-type receptor showed that they were almost identical, and the following amino acid residues were common for them: Gly87, Tyr88, Glu172, Glu175, Pro415, Ile417, Pro418, Asn419, and Thr420. The value of the Score for TiO_2 is (4138), which almost equaled the value of this parameter for the binding site of ZnO NP. On the contrary, the value of the Area and the ACE for TiO_2 NPs decreased, as compared with those of ZnO NPs, amounting to 526.50 $Å^2$ and 14.65 kJ/mol, respectively.

The comparison between the binding sites of both NPs and the extracellular part of the muscarinic choline M2-type receptor and the binding site of the acetylcholine mediator (amino acid composition of the site: Asp103, Tyr104, Ser107, Asn108, Trp155, Ala194, Trp400, Tyr403, Asn404, Cys429, and Tyr430) demonstrated that ZnO or TiO_2 NPs and acetylcholine did not compete for the binding sites on the receptor. However, the molecular docking showed the possibility for both NPs to form these bonds with some amino acids of the binding site LY2119620—an allosteric modulator of the muscarinic choline M2-type receptor (amino acid composition of the site: Tyr80, Tyr83, Glu172, Tyr177, Asn410, Asn419, Trp422, and Tyr426), which would impact the affinity between orthosteric ligands to this receptor and indicate the possibility of blocking the access of the agonist to its binding site by TiO_2 and ZnO NPs.

Then, the molecular docking of the spherical ZnO NP and the muscarinic choline M3-type receptor was performed. The binding site and its environment included seven amino acid

https://doi.org/10.1021/acsomega.1c02981
ACS Omega 2021, 6, 23960−23976

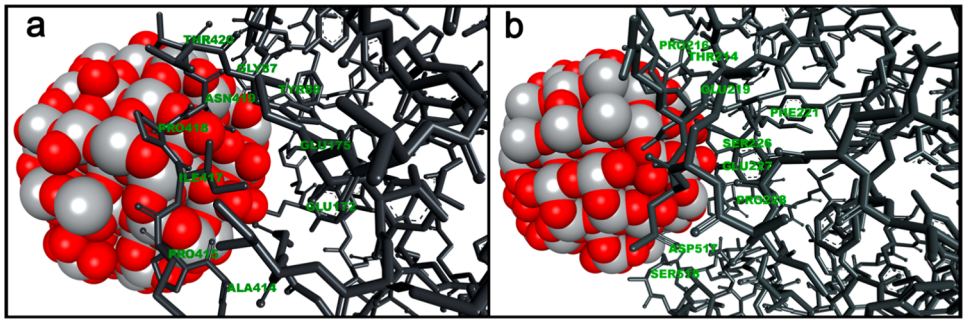

Figure 11. (a) Site of TiO_2 NP binding to the M2 muscarinic receptor; (b) site of TiO_2 NP binding to the M3 muscarinic receptor.

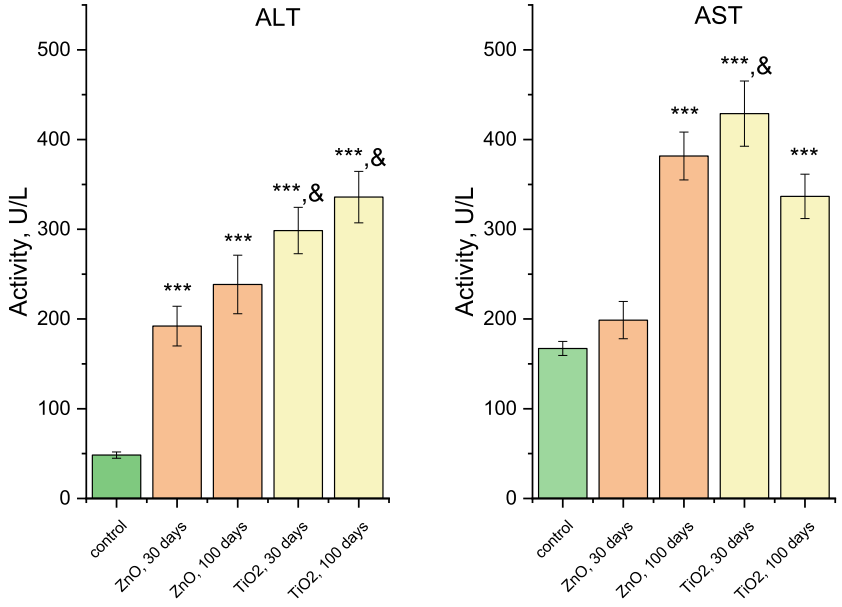

Figure 12. Activity of alanine aminotransferase (ALT) and aspartate aminotransferase (AST) in the blood plasma of rats in the control group and under the chronic impact of aqueous ZnO and TiO_2 nanocolloids in vivo for 30 and 100 days ($n = 7$); $^{***}p < 0.001$ as compared with the control and $^{\&}p < 0.05$ as compared with aqueous ZnO nanocolloids.

residues (Figure 11a); their ratio in terms of polarity was 0.43:0.14:0.43, and the respective distribution of the Gibbs free energy (kJ/mol) was (−0.77), (−0.41), and (−0.69). The values of the Score, Area, and ACE for this binding site were as follows: 4214, 558.60 Å^2, and 52.98 kJ/mol, respectively. The molecular docking of the spherical TiO_2 NP with the muscarinic M3-type receptor resulted in a slight increase in the number of amino acid residues (nine amino acid residues), as compared with the binding sites for ZnO NPs (Figure 11b), and their ratio in terms of polarity was 0.33:0.33:0.33. In addition, the comparison of the sites of binding two NPs with the muscarinic choline M2-type receptor demonstrated that the following amino acid residues were common for them: Thr214, Glu219, Phe221, Ser226, Glu227, Asp517, and Ser518. The corresponding distribution of the Gibbs free energy (kJ/mol) for the site of TiO_2 binding with the receptor was (−0.77), (5.65), and (−0.69). There was a slight increase in the Score and the Area, with their values reaching 4488 and 595.50 Å^2, respectively. On the contrary, the ACE value decreased to 48.87 kJ/mol. The binding sites of ZnO NPs and TiO_2 NPs and the extracellular part of the muscarinic choline M3-type receptor were compared with the binding site of acetylcholine (amino acid composition of the site: Asp147, Tyr148, Ser151, Asn152, Ala238, Trp503, Tyr506, Tyr529, and Cys532). The comparison showed that they did not compete with this mediator for the binding sites.

Study of Biochemical Markers for the Liver Function of Rats Burdened with ZnO and TiO_2 ANs (Comparison Performed Using Previous Data[36,46]). In our work, the activities of the enzymes of aminotransferase in blood plasma and the activity of ATPases in the preparations of plasmatic membranes of erythrocytes as well as the concentrations of direct, indirect, and conjugated bilirubin and the concentration of free and conjugated biliary acids in blood plasma were studied using the blood of three groups of rats: the control group ($n = 6$) and two groups of animals (six animals in each), which were burdened for 30 and 100 days with an aqueous nanocolloid of ZnO, respectively.

It is known[36,37] that the dominating pathway for xenobiotics to penetrate the systemic blood flow with subsequent spreading to tissues and organs is the hepatic portal system. Large particles (~500 nm) are mainly phagocytized by Kupffer cells (hepatic macrophages). If the particles have a size equal to or smaller than the size of hepatic sinusoids, they penetrate Disse's space easily and may be captured by hepatocytes. Later on, these particles may penetrate bile ducts along with bile or get back to the blood flow. It was also demonstrated[38] that the hepatotoxic action—inflammation, histopathological changes

https://doi.org/10.1021/acsomega.1c02981
ACS Omega 2021, 6, 23960−23976

in the liver structure, and its functional activity (increase in the level of alanine aminotransferase, low-density lipoproteins, decrease in glutathione concentration in blood plasma, etc.)—is caused by nanocolloids of ZnO (nanorods) after their intra-abdominal administration. When the organism is burdened with ZnO nanocolloids, there are impaired functions of the liver and other internal organs.[39−41] Taking the above-mentioned factors into consideration, we studied the functioning of liver cells of rats burdened with orally administered ZnO AN.

It is known that there is an increase in the activity of some transaminases in blood plasma when the liver tissue is being destroyed. In the first stage of our study, we determined the activity of these marker enzymes in the blood plasma of animals. Under the chronic intragastric introduction of aqueous ZnO nanocolloids, there was a considerable increase in the activity indices for alanine aminotransferase (ALT) and aspartate aminotransferase (AST) enzymes. Their activity in the control group of rats was as follows (in U/L): ALT, 48.4 ± 3.5; and AST, 167.2 ± 7.8 (n = 7). During the 30 day long intragastric introduction of aqueous ZnO nanocolloids, there was an increase in ALT and AST indices up to 192.1 ± 22.1 and 198.8 ± 20.8 U/L, respectively. During the 100 day long introduction of aqueous ZnO nanocolloids, there was a further increase in enzymatic activities: ALT, 238.5 ± 32.6 U/L; and AST, 381.7 ± 26.7 U/L (in all cases $p < 0.001$ regarding the control; n = 7) (Figure 12). It is noteworthy that the difference between the data of the ALT activity in the experimental groups (30 and 100 days) demonstrates no statistically significant changes.

Aminotransferases, represented by ALT and AST, transfer amino groups from 2-amino acid to 2-oxoacid involving pyridoxal phosphate as a cofactor. A significant increase in the activity of ALT and AST in the blood plasma demonstrates the process of hepatocyte lysis, which is one of the main pathological syndromes of liver damage.

Usually, besides liver tissue damage, the increase in the activity of the mentioned transaminases (especially AST) may show the destruction of cells in cardiac and skeletal muscles.[42] The index used to determine the cytotoxicity direction is the De Ritis ratio, which is the ratio between the activity of AST and ALT.[36,43] The oral exposure of rats to aqueous ZnO nanocolloids induced a decrease in this parameter. For animals burdened with the nanomaterial for 30 days, the De Ritis index decreased three times on average compared to the control, from 3.45 ± 0.16 to 1.03 ± 0.11. This parameter was twice below the control (1.60 ± 0.13) in the group of animals receiving ZnO ANs for 100 days. Thus, it is possible to state that a reliable decrease in the De Ritis index in the presence of ZnO in the organism indicated damage of the liver tissue.[36,43,44] It is noteworthy to mention that under longer burdening with ZnO ANs, there was a decrease in this index, which allowed forecasting a decrease in its cytotoxicity. This assumption was indirectly confirmed by the results of Sizova et al.,[45] who showed a considerable decrease in histological and biochemical impairments in the structure and function of the liver of rats when the duration of the impact of ZnO AN was prolonged.

***Comparison** of Changes in Parameters.* ALT and AST activity and the De Ritis index in the blood plasma of rats burdened with ZnO and TiO_2 ANs. The duration of burdening was 30 days. Changes in parameters by direction: All parameters coincided. Changes in parameters by value: ALT, AST: The most considerable changes (enhancing) were observed when rats were burdened with TiO_2 AN; De Ritis: changes (inhibition) of 1 order. The duration of burdening was 100 days. Changes in parameters by direction: All parameters coincided. Changes in parameters by value: ALT, AST: The most considerable changes (enhancing) were observed when rats were burdened with TiO_2 AN. De Ritis: The most considerable changes (inhibition) were observed when rats were burdened with TiO_2 AN (Figure 12).

In the next stage, we also studied the bilirubin of blood, which is one of the main indices of pigment exchange and a highly informative parameter of the functional state of the liver. The direct bilirubin, the total bilirubin, and the indirect bilirubin concentrations measured in the blood plasma of rats from the control group were 2.84 ± 0.17, 8.96 ± 0.53, and 6.12 ± 0.32 μM, respectively (n = 7). Rats that orally received ZnO ANs for 30 days had an increase in the direct, indirect, and total bilirubin concentrations, which were found to be 4.54 ± 0.33, 7.28 ± 0.38, and 11.83 ± 0.89 μM, respectively (in all cases, $p < 0.001$ regarding the control group; n = 7). We found that the direct, total, and indirect bilirubin concentrations in the plasma of rats burdened with ZnO ANs for 100 days were 7.38 ± 0.47, 17.92 ± 0.98, and 10.54 ± 0.76 μM, respectively (in all cases, $p < 0.001$ regarding the control group; n = 7). Therefore, the indices of the bilirubin concentration remained at a higher level under the impact of ZnO NPs, which demonstrated hepatotoxicity of their nanocolloids, but no time dependence was observed. A significant increase in the bilirubin concentration in the blood plasma of the animals under these conditions showed considerable destruction of liver parenchyma, which allowed bilirubin to penetrate the blood.

Comparison of changes in the parameters: concentrations of direct, total, and indirect bilirubin in the blood plasma of rats burdened with ZnO and TiO_2 ANs. The duration of burdening was 30 and 100 days. Changes in parameters by direction: All parameters coincided. Changes in parameters by value: The changes (enhancing) in all parameters were the values of the same order (the concentration of the total bilirubin in the blood plasma of rats burdened with ZnO AN for 30 days remained within the control range).

The thymol test is a marker of the mesenchymal inflammatory process in the liver. The result of the thymol test depends on the content of β- and γ-globulins in the blood serum and the inhibiting ability of β-lipoproteins of the blood serum. We performed the thymol test, and the analysis of its results demonstrated an increase in its indices. They reached the values expressed in related units as 0.95 ± 0.12 for the control group and (3.3 ± 0.2) and (3.7 ± 0.25) under the impact of ZnO ANs for 30 days and 100 days, respectively. Thus, the results obtained demonstrate that ZnO ANs are hepatotoxic, and under the chronic effect of NPs, they cause the impairment of protein and pigment exchange in the liver.

Comparison of changes in the parameters: the thymol test of blood serum of rats burdened with ZnO and TiO_2 ANs. The duration of burdening was 30 and 100 days. Changes in parameters by direction: All parameters coincided. Changes in parameters by value: The changes (enhancing) in all parameters were the values of the same order.

Study of the Exchange of Biliary Acids in Rats Burdened with Nanocolloids of ZnO and TiO_2 (Comparison Performed Using Previous Data[46]). Along with the indices of the enzymatic activity of ALT and AST, a

https://doi.org/10.1021/acsomega.1c02981
ACS Omega 2021, 6, 23960−23976

sensitive index of liver function is the concentration of biliary acids in the blood plasma.[42,44] Thus, since our previous studies demonstrated a considerable impairment in the protein and pigment exchange in the liver of rats under the impact of ZnO nanocolloids in vivo, our further experiments were related to the analysis of the exchange of biliary acids in rats burdened with the ZnO nanocolloids for 30 days. Using the method of liquid thin-layer chromatography, we studied the composition of conjugated (TCA, taurocholic acid; the mixture of TCDCA, taurochenodeoxycholic acid, TDCA, taurodeoxycholic acid; GCA, glycocholic acid; the mixture of GCDCA, glycochenodeoxycholic acid; and GDCA, glycodeoxycholic acid) and free (CA, cholic acid; the mixture of CDCA, chenodeoxycholic acid; and DCA, deoxycholic acids) biliary acids in the blood plasma of rats. It was determined that with oral intake of ZnO ANs for 30 days, there were considerable changes in the concentration of the abovementioned biliary acids in the blood plasma of the rats, namely, a reliable increase in the concentration of free CA, while the concentrations of other conjugated and free biliary acids decreased by 30−50% on average (Figure 13).

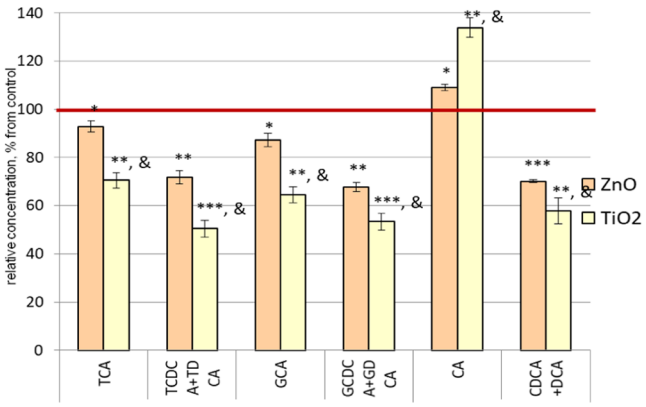

Figure 13. Relative concentration (in % regarding the corresponding control values) of the conjugated and free biliary acids in the blood plasma of rats burdened with ZnO and TiO_2 ANs for 30 days ($n = 6$). Legends: TCA, taurocholic acid; TCDCA, taurochenodeoxycholic acid; TDCA, taurodeoxycholic acid; GCA, glycocholic acid; GCDCA, glycochenodeoxycholic acid; GDCA, glycodeoxycholic acid; CA, cholic acid; CDCA, chenodeoxycholic acid; DCA, deoxycholic acid. * $p < 0.05$; ** $p < 0.01$, *** $p < 0.001$ for the control group and $^{\&}p < 0.05$ for the experiments with rats burdened with ZnO AN.

It is known[39,46] that ZnO NPs are capable of accumulating in hepatocytes, inhibiting the expression of antioxidant protection genes (superoxide dismutase, glutathione peroxidase, and catalase), increasing the rate of anti-inflammatory factors (TNF-α and IL-6), and enhancing the expression of proapoptotic genes (p53); a considerable fragmentation of hepatocyte DNA takes place under the same conditions. In particular, Tang et al.[41] determined that burdening rats with ZnO nanocolloids was accompanied by the impairment of the expression of genes encoding specific enzymes of the P450 superfamily; it is known[47] that these enzymes ensure the metabolism of bilirubin and biliary acids. One of the central aspects of the toxic impact of ZnO nanocolloids on cells is the impairment of mitochondria functioning.[48] Taking the abovementioned factors into consideration, it is possible to assume that the decrease in the concentration of free and conjugated fatty acids in the blood plasma of rats burdened with ZnO nanocolloid, determined in our experiments under these conditions, may be related to the changes in the level of enzymes in the liver, which ensure the synthesis and transformation of biliary acids.

Comparison of changes in the parameters: concentrations of free and conjugated biliary acids in the blood plasma of rats burdened with ZnO and TiO_2 ANs. The duration of burdening was 30 days. Changes in parameters by direction: All parameters coincided. Changes in parameters by value: The changes (decrease, except for an increase in free cholic acid) in all parameters were the values of approximately the same order.

Study of the Activity of ATPases of Plasma Membranes of Blood Erythrocytes of Rats Burdened with ZnO and TiO_2 ANs (Comparison Performed Using Previous Data[46]). The systems of primary active ion transport in the blood plasma of the cell ensure the maintenance of transmembrane difference in the concentrations of Na^+, K^+, and Ca^{2+} ions. It is known that impairment in the transport function of active ionic transport systems may cause different effects, including apoptosis or mixed processes of cell death.[49,50] In the next series of experiments, we studied the indices of total Mg^{2+}-dependent, ouabain-sensitive, and ouabain-insensitive ATPase activities of the preparations of blood plasma erythrocytes.

In the control, the indices under investigation were as follows (in mg Pi/(mg protein per h)): 1.64 ± 0.05, 0.85 ± 0.06, and 0.79 ± 0.05 for the total Mg^{2+}-dependent ATPase, ouabain-sensitive, and ouabain-insensitive activities, respectively. Therefore, the activity of Na^+ and K^+-ATPase for blood plasma erythrocytes of rats was 51.8% on average compared to the total ATPase activity, accepted as 100%. During the chronic impact of aqueous ZnO nanocolloids, the activity of enzymes of the primary active ion transport decreased as compared to the control. The indices of total Mg^{2+}-dependent, ouabain-sensitive, and ouabain-insensitive ATPase activities for rats burdened with ZnO ANs for 30 days were as follows (in mg Pi/(mg protein per h)): 1.19 ± 0.02, 0.57 ± 0.01, and 0.62 ± 0.02 ($n = 6$; in all cases, $p < 0.05$ with respect to the control values), respectively. In the group of rats with 100 days of exposure to ZnO ANs, there was a further decrease in the activity of total Mg^{2+}-dependent, ouabain-sensitive, and ouabain-insensitive ATPases, the values of which were as follows (in mg Pi/(mg protein per h)): 0.8 ± 0.01, 0.48 ± 0.01, and 0.32 ± 0.01 ($n = 6$; in all cases, $p < 0.05$ regarding the control values), respectively. While analyzing these data, it should be noted that there was a decrease in the relative contribution of Na^+ and K^+-ATPase in the total Mg^{2+}-dependent ATPase activity of erythrocyte PM under the effect of aqueous ZnO nanocolloids in vivo: in the group of animals treated for 30 days, these parameters were 47.6% on average, and in the group of animals, treated for 100 days, these parameters were 60.0% on average.

***Comparison** of Changes in the Parameters.* Mg^{2+}-dependent, ouabain-sensitive, and ouabain-insensitive ATPase activities of plasma membranes of blood erythrocytes of rats burdened with ZnO and TiO_2 ANs. The duration of burdening is 30 and 100 days. Changes in parameters by direction: All parameters coincided. Changes in parameters by value: The most considerable changes (inhibition) in the activity of ouabain-sensitive ATPase were observed when rats were burdened with TiO_2 AN for 100 days. Therefore, long-term systemic in vivo intake of TiO_2 and ZnO ANs causes considerable inhibition of the systems of primary active ion

https://doi.org/10.1021/acsomega.1c02981
ACS Omega 2021, 6, 23960−23976

transport via the plasmatic membrane of the cells, which may be one of the primary mechanisms causing pathological changes in animals under the impact of these nanocolloids.

Recent studies have shown that nanomaterials of metals and their oxides, in particular ZnO and TiO_2, when get into the organism, have a pro-oxidant and proinflammatory effect.[51−54] In particular, as shown by Nogueira and colleagues,[53] a relatively short (10 days) intragastric administration of a TiO_2 suspension to mice causes inflammatory processes in the intestine, which are accompanied by an increase in the level of proinflammatory factors: interleukins (ILs 1β, 4, 6, 8, 10, 12, 13, 17, 23), tumor necrosis factor α (TNF-α), and γ interferon; an increased level of infiltration with T (CD4+) lymphocytes was also found in the intestinal walls. According to Bettini et al.,[54] chronic use of TiO_2 NP suspension for 100 days in an amount of 200 mg/day by Wistar rats was accompanied by an increase in the level of certain proinflammatory cytokines (IL-6, TNF-α, IL-8, and IL-10) in the mucous membrane of the large intestine. Cell survival under conditions of incubation with TiO_2 nanoparticles depends on the level of expression of detoxifying and antioxidant enzymes in these cells.[54,55]

A number of studies have shown that TiO_2 NPs accumulate in significant amounts in liver tissues and cause an inflammatory reaction and cell damage there when taken orally.[18,36,56,57] In particular, as evidenced by the data of Abbasi-Oshaghi et al.,[57] oral administration of TiO_2 NPs to rats for 30 days (rutile polymorph, average particle size is 30 nm, and doses used are 10−100 mg/kg per day) caused a significant increase in the activity of ALT and AST, as well as the concentration of bilirubin in the blood plasma against the background of increased apoptosis of hepatocytes and significant suppression of the expression of genes encoding antioxidant defense enzymes. Jia et al.[58] showed that oral administration of TiO_2 NPs to mice for 14 days (polymorph anatase; particle sizes: 5, 10, 60, and 90 nm; and doses used are 5−50 mg/kg per day) caused a number of histotoxic reactions; in particular, in the liver tissue, it was accompanied by damage of mitochondria and activation of apoptosis and general impairment of glucose and lipid metabolism. It is interesting that under these conditions, disturbances in the activities of acetylcholine esterase and nitric oxide synthase (both constitutive and inducible isoforms) were observed in the brain tissues.

Therefore, the in vivo effects of high doses of nano-TiO_2 on liver function have been extensively studied, while similar information on the study of the effect of ZnO NPs administered orally is much more limited, but the available data indicate the cytotoxic (in particular, hepatotoxic) effect of this nanomaterial, the main mechanism of which is the activation of oxidative stress in cells.[59−61] Thus, the results of studies by Aboulhoda et al.,[59] in which ZnO NPs (size about 7 nm, doses used 100−300 mg/kg per day) were orally applied to Sprague−Dawley rats for 14 days, showed the activation of oxidative stress, apoptosis, and hepatotoxicity of nano-ZnO. Using female mice, Esmaeillou et al.[60] showed that oral intake of nano-ZnO (dimensions about 20−30 nm, used doses are 333.33 mg/kg per day) is accompanied by significant structural and functional disorders of the tissues of the liver, kidneys, lungs, and genitals; in particular, animals were characterized by a significant (by a quarter of the control) decrease in the thickness of the myometrium and had a significant increase in the activities of ALT and AST in the blood plasma.

Therefore, at the moment, a significant amount of data that indicate the cytotoxicity (and, in particular, hepatotoxicity) of nanosized materials of ZnO and TiO_2 has been accumulated. However, the information available in the scientific literature about in vivo studies mainly concerns the determination of the effects of high doses of these nanomaterials (tens and hundreds of mg/kg) and mainly under conditions of intraperitoneal, intravenous, or inhalation introduction into the organism of laboratory animals. In our study, for the first time, the patterns and mechanisms of action of the ZnO AN (in a comparative aspect with nano-TiO_2) with prolonged oral intake into the body in doses, which in terms of mg/kg correspond to the increased doses that a person receives in domestic conditions (with food products, cosmetics and hygiene products, medicines, medicines), were established.[64,65]

CONCLUSIONS

The TEM/HRTEM methods were used in our work to confirm the application of the colloid solutions of zinc hydroxide/zinc oxide core−shell nanoparticles (ZnO nanocolloid), which differ from the solutions of Zn^{2+} ions, zinc complexes. As expected, the hydrophilicity of the shell prevents the encapsulated crystalline ZnO/β-$Zn(OH)_2$ core from dissolution in water. It is also shown that the outer shell of hydrolyzed semiamorphous titanium dioxide covers the nanocrystalline core of TiO_2 in AN. Hydroxylation, as any surface modification, aims at protection of TiO_2 NPs in media of different acidities. In this work, a difference in the values of mechanokinetic parameters of the smooth muscle spontaneous contractions of the antrum and cecum of the rats' large intestine was shown by the tensometric method in the isometric mode. The indices of the work efficiency of these muscles were also different and acquired a higher value in the antrum SM. The studies demonstrated that the burdening of the rats with ZnO AN for 30 days was accompanied by an impairment in the processes of regulating the GIT motility. We observed a narrowing of the amplitude range, a decrease in frequency of spontaneous contractions, and the inhibition of efficiency indices for the work of SMs of the antrum and cecum. Under longer (100 days) burdening of rats with ZnO AN, there was a tendency toward restoring AU indices, as seen by the decrease in the effects of its impact on spontaneous contractions of SMs. In terms of the value and the direction of changes in most parameters of spontaneous contractions of SMs, the effect (for 30 days) of the TiO_2 AN differed from that for ZnO AN and was almost the same under their longer impacts. It was also found that during the cholinergic excitation of SMs in the GIT, the sensitivity to the effect of ZnO AN was demonstrated by M3- and M2-receptor-dependent mechanisms of regulating the intracellular concentration of Ca^{2+} ions with the prevalence of the effect of this nanomaterial on M2-receptor-dependent mechanisms of the intake of extracellular Ca^{2+} ions into SMC via voltage-gated Ca^{2+} channels of L-type. Under these conditions, the effects of TiO_2 AN on these regulatory mechanisms were much smaller in terms of the value and opposite in their direction. The performed molecular docking of muscarinic acetylcholine M3- and M2-type receptors with ZnO and TiO_2 NPs demonstrated that their binding sites were almost identical and did not compete with acetylcholine for the binding sites. At the same time, the presented studies demonstrated the possibility of forming bonds between NPs and some amino acids of the binding site LY2119620—an allosteric modulator of M2

https://doi.org/10.1021/acsomega.1c02981
ACS Omega 2021, 6, 23960−23976

cholinoreceptor, which would impact the affinity of orthosteric ligands to this receptor and indicate the possibility of blocking the access of the agonist to its binding sites by ZnO and TiO_2 NPs.

The abovementioned changes in the parameters of spontaneous contractions and contractions of SMs caused by acetylcholine, high-potassium Krebs solution after burdening the rats with ZnO nanocolloid for 30 days coincide in the direction (except for changes in the frequency of spontaneous contractions). However, they differ in the value of parameters in different parts of the GIT. These differences diminish significantly with a longer influence. Under the same conditions of burdening rats with a TiO_2 AN (30 and 100 days) in various parts of the gastrointestinal tract, it is shown that a number of parameters are insensitive to the action of this nanomaterial, and those parameters that change reach the values of the same order (with the exception of the index of the effectiveness of the work of smooth muscle and the range of amplitudes).

Studies of the condition of the hepatobiliary system of rats burdened with ZnO and TiO_2 ANs demonstrated that impairments of the cellular metabolism caused by burdening were accompanied by changes (inhibition or hyperstimulation) in the activity of both intracellular enzymes and the ion transport (for Na^+, K^+, and Ca^{2+} systems) through the plasma membrane of hepatocytes. The ionic gradient formed in this case is known[62,63] to be related to bile secretion processes. The impairment in these inter-related processes on hepatocyte membranes is likely to be among the reasons for the manifestation of the toxic effect of ZnO and TiO_2 ANs on the hepatobiliary system of rats. The effects of the stated ANs under these conditions were the same in terms of the direction of changes in the parameters but different in terms of their scale.

MATERIALS AND METHODS

In the experiments in vivo, the use of 8 week old Wistar rats of both genders was involved. These rats were kept in standard conditions of the vivarium (at room temperature of 20 ± 2 °C, relative humidity of 50−70%, and light−darkness cycle of 12:12 h). The intragastric dose of aqueous ZnO nanocolloids (in terms of 3 mg/kg/day of dry matter) was selected under the protocol[64,65] regarding the probable daily limits of this nanomaterial, which can cause toxic manifestations, > 50 mg/person/day or 0.7 mg/kg/day, calculated as per a weight unit. Controlling the bodyweight of rats was performed every 4−6 days.

The experiments in vitro were conducted using isolated preparations, namely, circular smooth muscle (SM) stripes of the cecum and the antrum of rats. The registration of spontaneous contractile activity was conducted using the tenzometric method in the isometric mode; further on, we studied such parameters as the frequency of preparation contractions for 10 min, the averaged value of the duration of the contraction−relaxation cycle, the duration of some contraction fragments, the asymmetry coefficient, and the Alexandria (AU) index of contractions.[66]

The animal experiments were conducted under the guidelines of the European Convention for the Protection of Vertebrate Animals used for Experimental and Other Scientific Purposes (Strasbourg, 1986).

The normal Krebs solution with the following concentration of constituents (in mM) was used in the experiments: NaCl, 120.4; KCl, 5.9; $NaHCO_3$, 15.5; NaH_2PO_4, 1.2; $MgCl_2$, 1.2; $CaCl_2$, 2.5; glucose, 11.5; pH 7.4. The high-potassium Krebs solution with the concentration of K^+ ions (80 mM) was prepared by replacing the required amount of Na^+ ions in the normal Krebs solution with an equimolar amount of K^+ ions. Nominally, a calcium-free Krebs solution was prepared by replacing $CaCl_2$ with an equimolar amount of NaCl. Acetylcholine (AC, Sigma, USA) was used at the concentration of 10^{-5} mol/L.

The biochemical markers of damage and functional ability of the liver (activity of alanine aminotransferase and aspartate aminotransferase) under the long-term exposure of the organism to ZnO aqueous nanocolloids (ANs) were studied on preparations of blood plasma and a suspension of rat erythrocyte plasma membranes (PMs). Blood with an anticoagulant (heparin, 5000 IU/mL) at a blood/heparin ratio of 9:1 was centrifuged at 3000 rpm for 10 min. Plasma was isolated with a pipette and further kept for a short period of time (12−24 h) at 4 °C until being used in the experiments for determining the activity of alanine aminotransferase (ALT) and aspartate aminotransferase (AST), bilirubin concentration, and the thymol test. The precipitation (blood corpuscles) was further used to obtain the preparations of erythrocyte plasma membranes.

To determine the activities of AST and ALT in the blood plasma of rats by the Reitman−Fresnel method,[67] to find the total and direct bilirubin by the standard Endrashik method,[68] and to conduct the thymol turbidity test,[69] we used test kits (R&D enterprise Felicity-Diagnostics, Ukraine). Free and conjugated biliary acids in the blood plasma of rats were isolated and determined by the method described in ref 70.

The functioning of the systems of primary active ion transport in PM was studied on the preparations of an erythrocyte PM suspension, which was obtained by the slightly modified Dodge's method. The protein concentration in the preparation of the erythrocyte PM of rats was determined by Lowry's method.[71] Total Mg^{2+}, Na^+, and K^+-ATPase activity was determined in the fraction of erythrocyte PMs in 0.4 mL of the standard incubation medium at 37 °C. This incubation medium contained (in mM) 1 ATP, 3 $MgCl_2$, 125 NaCl, 25 KCl, 1 EGTA, 20 Hepes-Tris-buffer (pH 7.4), and 1 NaN_3 (inhibitor of mitochondria ATPase).[61] A 0.1 μM of thapsigargin (the selective inhibitor of Ca^{2+}, Mg^{2+}-ATPase of the endo(sarco)plasmatic reticulum) and a 0.1 μM of 0.1% digitonin (the factor of PM perforation) were added to the incubation medium. In the membrane fraction of the sample, the protein amount was 20−30 μg, and the incubation period lasted for 4 min. The enzymatic reaction was initiated by the introduction of the aliquot (20 μL) of the PM suspension to the incubation medium, and it was terminated by the introduction of 1 mL of 20% trichloroacetic acid (pH 4.3 at 8 °C) to the incubation mixture. An incubation medium with a similar composition but lacking fragments of PMs served as the "control" for the nonenzymatic hydrolysis of ATP. The aqueous solution of the membranes served as the "control" for the amount of endogenous Pi (inorganic phosphorus) in the membrane preparation. Thus, the total ATPase activity was calculated as the difference between the amount of Pi formed in the incubation medium with and without PMs. The amount of Pi reaction product was determined in the supernatant by the method of Rathbun and Betlach.[72] In the experiments, the Mg^{2+}-ATPase activity determined in the incubation medium was used for the total ATPase activity measurements, in the

https://doi.org/10.1021/acsomega.1c02981
ACS Omega 2021, 6, 23960−23976

presence of 1 mM ouabain, a selective inhibitor of Na^+, K^+-ATPase. The ouabain-sensitive Na^+, K^+-ATP activity was calculated as the difference between the total Mg^{2+}, Na^+, K^+-ATPase and the ouabain-insensitive Mg^{2+}-ATPase activity.[73]

Commercial nanomaterial: Ultradispersed ZnO powder (PlasmaChem GmbH, Berlin, Germany) was used in the work. The specific surface area of ZnO was 19 ± 5 m^2/g, purity was > 99.5%, and the average primary particle size of NPs was about 25 nm. For comparison, a commercial nanomaterial (Nanoparticles, type P25) of ultradispersed TiO_2 powder was purchased from the same source. Dry nanopowder was composed of a mixed rutile/anatase phase with an average primary particle size of 21 ± 5 nm, SSA of 50 ± 10 m^2/g, purity > 99.5%, and moisture below 1.5%.

X-ray powder diffraction (XRPD) patterns were recorded in a $\theta-2\theta$ mode on a Shimadzu XRD-6000 diffractometer using Cu Kα radiation (λ = 1.5405 Å). Qualitative analysis was performed by the JCPDS database for phase identification and to provide information on unit cell dimensions.

To study the effect of ZnO NP hydrolysis using transmission electron microscopy/high-resolution transmission electron microscopy (TEM/HRTEM) and related methods, we prepared the ZnO nanocolloids in water as follows: 25 mg of commercial ZnO NPs was dispersed in 10 mL of deionized water in a thin polypropylene cup. This cup was placed inside an ultrasonic horn (set at 100 W) and then subjected to 28 kHz sonication for 10 minutes, incubated for 8 hours, and then sonicated again, immediately before TEM investigation.

A total of 10 μL of the prepared nanocolloids was dropped onto carbon-coated copper TEM microgrids, allowing the solvent to evaporate in a vacuum chamber. As a reference, we took the same quantity of ZnO NPs and prepared nanocolloids, as reported above, in abs. ethanol immediately before TEM studies.

TEM and HRTEM images were collected on a JEOL JEM-2100F microscope, equipped with a Schottky FEG and operating at an accelerating voltage of 200 kV. The JEOL 2100F microscope was also equipped with a Gatan Orius SC200D ($2k \times 2k$) diffraction camera and a GIF TRIDIEM postcolumn energy filter for the acquisition of energy-filtered images and selected area electron diffraction (SAED) studies.

This paper presents a statistical analysis of experimental data obtained in the study and processed by variation statistics methods using Origin Pro 8 software. The samples were checked to belong to normally distributed general populations, according to the Shapiro–Wilk criterion. Dispersion analysis was used to determine reliable differences between the mean values of samplings, and the post-test comparison was made using the Tukey test. In all cases, the results were reliable provided the probability value p was less than 5% ($p < 0.05$). The obtained results were presented as the arithmetic mean ± standard error of the mean value, and the n value was determined by the total number of experiments.

■ ASSOCIATED CONTENT

Supporting Information

The Supporting Information is available free of charge at https://pubs.acs.org/doi/10.1021/acsomega.1c02981.

PXRD pattern of ZnO and TiO_2 NPs; TEM images and SAED patterns of HT/TiO_2 NPs (PDF)

■ AUTHOR INFORMATION

Corresponding Author

Valeriy Skryshevsky − *Institute of High Technologies, Taras Shevchenko National University of Kyiv, 01033 Kyiv, Ukraine; Corporation Science Park Taras Shevchenko University of Kyiv, 01033 Kyiv, Ukraine;* orcid.org/0000-0003-0249-5556; Email: skrysh@univ.kiev.ua

Authors

Olga Tsymbalyuk − *Institute of High Technologies, Taras Shevchenko National University of Kyiv, 01033 Kyiv, Ukraine*

Tamara Davydovska − *Institute of High Technologies, Taras Shevchenko National University of Kyiv, 01033 Kyiv, Ukraine*

Vladyslav Lisnyak − *Chemical Faculty, Taras Shevchenko National University of Kyiv, 01033 Kyiv, Ukraine; Prešov University in Prešov, 081 16 Prešov, Slovakia;* orcid.org/0000-0002-6820-1445

Stanislav Veselsky − *Institute of High Technologies, Taras Shevchenko National University of Kyiv, 01033 Kyiv, Ukraine*

Alexander Zaderko − *Institute of High Technologies, Taras Shevchenko National University of Kyiv, 01033 Kyiv, Ukraine; Corporation Science Park Taras Shevchenko University of Kyiv, 01033 Kyiv, Ukraine;* orcid.org/0000-0002-8174-1470

Ivan Voiteshenko − *Institute of High Technologies, Taras Shevchenko National University of Kyiv, 01033 Kyiv, Ukraine*

Anna Naumenko − *Institute of High Technologies, Taras Shevchenko National University of Kyiv, 01033 Kyiv, Ukraine*

Complete contact information is available at: https://pubs.acs.org/10.1021/acsomega.1c02981

Author Contributions

The manuscript was written through contributions of all authors. All authors have given approval to the final version of the manuscript.

Notes

The authors declare no competing financial interest.

■ ACKNOWLEDGMENTS

This work was partially supported by the EU Horizon 2020 Research and Innovation Staff Exchange Programme (RISE) under the Marie Skłodowska-Curie Action (project 101008159 "UNAT") and the Ministry of Education and Science of Ukraine (project 0119U100326). The authors thank LLL Novations for their guidance on working with the nanomaterials.

■ ABBREVIATIONS

AC, acetylcholine; ALT, alanine aminotransferase; AN, aqueous nanocolloid; AST, aspartate aminotransferase; AU, Alexandria units; CA, cholic acid; DCA, deoxycholic acids; GCA, glycocholic acid; GCDCA, glycochenodeoxycholic acid; GDCA, glycodeoxycholic acid; GIT, gastrointestinal tract; HKS, high-potassium Krebs solution; HRTEM, high-resolution transmission electron microscopy; ICC, interstitial cells of Cajal; IP_3, inositol-1,4,5-triphosphate; NPs, nanoparticles; PM, plasma membranes; ROS, reactive oxygen species; SAED,

selected area electron diffraction; SC, spontaneous contractions; SMs, smooth muscles; TCDCA, taurochenodeoxycholic acid; TDCA, taurodeoxycholic acid; TEM, transmission electron microscopy; VGC, voltage-gated Ca^{2+} channels

REFERENCES

(1) Wang, X.; Song, J.; Wang, Z. L. Nanowire and nanobelt arrays of zinc oxide from synthesis to properties and to novel devices. *J. Mater. Chem.* **2007**, *17*, 711−720.

(2) Lee, Y. J.; Ahn, E. Y.; Park, Y. Shape-dependent cytotoxicity and cellular uptake of gold nanoparticles synthesized. *Nanoscale Res. Lett.* **2019**, *14*, No. 129.

(3) Naeem, F.; Naeem, S.; Zhao, Y.; Wang, D.; Zhang, J.; Mei, Y. F.; Huang, G. TiO_2 nanomembranes fabricated by atomic layer deposition supercapacitor with enhanced capacitance. *Nanoscale Res. Lett.* **2019**, *14*, No. 19.

(4) Fahmi, A.; Minot, C.; Silvi, B.; Cause, M. Theoretical analysis of the structure of titanium dioxide crystals. *Phys. Rev. B* **1993**, *47*, 11717−11724.

(5) Gusev, A. I. *Nanomaterials, Nanostructures, Nanotechnologies*; Moscow State University: Moscow, Ru, 2005.

(6) Wang, Z. L. Zinc oxide nanostructures: growth, properties and applications. *J. Phys.: Condens. Matter* **2004**, *16*, R829−R858.

(7) Nafees, M.; Liaqut, W.; Ali, S.; Shafique, M. A. Synthesis of ZnO/Al:ZnO nanomaterial: structural and band gap variation in ZnO nanomaterial by Al doping. *Appl. Nanosci.* **2013**, *3*, 49−55.

(8) Gyu-Chul, Y. *Semiconductor Nanostructures for Optoelectronic Devices. Processing, Characterization and Applications*; Springer, 2012.

(9) Averin, I. A.; Pronin, I. A.; Yakushova, N. D.; Karmanov, A. A.; Alimova, E. A.; Igoshina, S. E.; Moshnikov, V. A.; Terukov, E. I. Adaptation of sol-gel technology of nanostructured zinc oxide for the purposes of flexible electronics. *Zhurnal tekhnicheskoy fiziki* **2019**, *89*, 1917−1922.

(10) Multian, V. V.; Uklein, A. V.; Zaderko, A. N.; Kozhanov, V. O.; Boldyrieva, O. Y.; Linnik, R. P.; Lisnyak, V. V.; Gayvoronsky, V. Y. Synthesis, Characterization, Luminescent and Nonlinear Optical Responses of Nanosized ZnO. *Nanoscale Res. Lett.* **2017**, *12*, No. 164.

(11) Donnadio, A.; Cardinalli, G.; Latterini, L.; Roscini, L.; Ambrogi, V. Nanostructured zinc oxide on silica surface: Preparation, physicochemical characterization and antimicrobial activity. *Mater. Sci. Eng., C* **2019**, *104*, No. 109977.

(12) Sruthi, S.; Valappil Mohanan, P. Engineered zinc oxide nanoparticles; biological interactions at the organ level. *Curr. Med. Chem.* **2016**, *23*, 4057−4068.

(13) Pulit-Prociak, J.; Chwastowski, J.; Rodrigues, L. B.; Banach, M. Analysis of the physicochemical properties of antimicrobial compositions with zinc oxide nanoparticles. *Sci. Technol. Adv. Mater.* **2019**, *20*, 1150−1163.

(14) Pasquet, J.; Chevalier, Y.; Couval, E.; Bouvier, D.; Bolzinger, M. A. Zinc oxide as a new antimicrobial preservative of topical products: Interactions with common formulation ingredients. *Int. J. Pharm.* **2015**, *479*, 88−95.

(15) Moreno-Olivas, F.; Tako, E.; Mahler, G. J. ZnO nanoparticles affect intestinal function in an in vitro model. *Food Funct.* **2018**, *9*, 1475−1491.

(16) Shuba, M. F.; Vladimirova, I. A.; Philyppov, I. B. Mechanisms of the inhibitory action of neurotransmitters on smooth muscles. *Neurophysiology* **2003**, *35*, 224−232.

(17) Dryn, D. O.; Gryshchenko, A. V.; Bolton, T. B.; Zhu, M. X.; Zholos, A. V. Species-related differences in the properties of TRPC4 channels in intestinal myocytes of rodents. *Neurophysiology* **2016**, *48*, 220−229.

(18) Tsymbalyuk, O. V.; Naumenko, A. M.; Rohovtsov, O. O.; Skoryk, M. A.; Voiteshenko, I. S.; Skryshevsky, V. A.; Davydovska, T. L. Titanium dioxide modulation of the contractibility of visceral smooth muscles in vivo. *Nanoscale Res. Lett.* **2017**, *12*, No. 129.

(19) Naumenko, A. M.; Tsymbalyuk, O. V.; Skoryk, M. A.; Voiteshenko, I. S.; Skryshevsky, V. A.; Davydovska, T. L. Nanosized titanium dioxide material. Modulation of spontaneous motility and GABA-dependent regulation of functions of stomach smooth muscles in vivo. *Stud. Microbiol.* **2017**, *11*, 5−16.

(20) Yu, Z.; Li, Q.; Wang, J.; Yu, Y.; Wang, Y.; Zhou, Q.; Li, P. Reactive oxygen species-related nanoparticle toxicity in the biomedical field. *Nanoscale Res. Lett.* **2020**, *15*, No. 115.

(21) Kravtsov, A. A.; Blinov, A. V.; Yasnaya, V. A.; Sysoev, I. A.; Gish, E. A. Study of the influence of pH of the reaction medium on the acid-base properties of the surface of the TiO_2 nanoparticles, synthesized by sol-gel method. *Eng. Don Gaz.* **2015**, *1*, 2−16.

(22) Petrishyn, R. R.; Yaremko, Z. M.; Soltis, M. N. Influence of pH of the medium and surfactants on ζ - potential and aggregative stability of titanium dioxide. *Colloid. J.* **2010**, *72*, 512−517.

(23) Shi, H.; Magaye, R.; Castranova, V.; Zhao, J. Titanium dioxide nanoparticles: a review of current toxicological data. *Part Fibre Toxicol.* **2013**, *10*, No. 15.

(24) McConnell, E. L.; Basit, A. W.; Murdan, S. Measurements of rat and mouse gastrointestinal pH, fluid and lymphoid tissue, and implications for in vivo experiments. *J. Pharm. Pharmacol.* **2010**, *60*, 63−70.

(25) Furness, J. B.; Callaghan, B. P.; Rivera, L. R.; Cho, H. J. The enteric nervous system and gastrointestinal innervation: integrated local and central control. *Adv. Exp. Med. Biol.* **2014**, *817*, 39−71.

(26) Blair, P. J.; Rhee, P.-L.; Sanders, K. M.; Ward, S. M. The significance of interstitial cells in neurogastroenterology. *J. Neurogastroenterol. Motil.* **2014**, *20*, 294−317.

(27) Benarroch, E. E. Enteric nervous system: functional organization and neurologic implications. *Neurology* **2007**, *69*, 1953−1957.

(28) Torihashi, S.; Fujimoto, T.; Trost, C.; Nakayama, S. Calcium oscillation linked to pacemaking of interstitial cells of Cajal. *J. Biol. Chem.* **2002**, *277*, 19191−19197.

(29) Al-Shboul, O. A. The importance of interstitial cells of Cajal in the gastrointestinal tract. *J. Gastroenterol.* **2013**, *19*, 3−15.

(30) Cipriani, G.; Serboiu, C. S.; Gherghiceanu, M.; Faussone-Pellegrini, M. S.; Vannucchi, M. G. NK receptors, Substance P, Ano1 expression and ultrastructural features of the muscle coat in Cav-1(-/-) mouse ileum. *J. Cell Mol. Med.* **2011**, *15*, 2411−2420.

(31) Naota, M.; Shimada, A.; Morita, T.; Yamomoto, Y.; Inoue, K.; Takano, H. Caveolae − mediated endocytosis of intratracheally instilled gold colloid nanoparticles at the air-blood barrier in mice. *Toxicol. Pathol.* **2013**, *41*, 487−496.

(32) Mir, A. H.; Qamar, A.; Qadir, I.; Nagvi, A. H.; Begum, R. Accumulation and trafficking of zinc oxide nanoparticles in an invertebrate model, *Bombyx mori*, with insights on their effects on immune-competent cells. *Sci. Rep.* **2020**, *10*, No. 1617.

(33) Ratz, P. H.; Berg, K. M.; Urban, N. H.; Miner, A. S. Regulation of smooth muscle calcium sensitivity: KCl as a calcium sensitizing stimulus. *Am. J. Physiol.: Cell Physiol.* **2005**, *288*, C769−C783.

(34) Zholos, A. V.; Tsvilovskyy, V. V.; Bolton, T. B. Muscarinic cholinergic excitation of smooth muscle signal transduction and signal cationic channel properties. *Neurophysiology* **2003**, *35*, 283−301.

(35) Deng, J. T.; Van Lierop, J. E.; Sutherland, C.; Walsh, M. P. Ca^{2+}-independent smooth muscle contraction. A novel function for integrin-linked kinase. *J. Biol. Chem.* **2001**, *276*, 16365−16373.

(36) Tsymbalyuk, O. V.; Veselsky, S. P.; Naumenko, A. M.; Davydovska, T. L.; Voiteshenko, I. S.; Chyzh, I. I.; Skryshevsky, V. A. TiO_2 hepatotoxicity under long-term administration to rats. *Ukr. Biochem. J.* **2020**, *92*, 45−54.

(37) Baboci, L.; Capolla, S.; Di Cintio, F.; Colombo, F.; Mauro, P.; Dal Bo, M.; Argenziano, M.; Cavalli, R.; Toffoli, G.; Macor, P. The Dual Role of the Liver in Nanomedicine as an Actor in the Elimination of Nanostructures or a Therapeutic Target. *J. Oncol.* **2020**, 1−15.

(38) Moatamed, E. R.; Hussein, A. A.; El-Desoky, M. M.; Khayat, Z. E. Comparative study of zinc oxide nanoparticles and its bulk form on liver function of Wistar rat. *Toxicol. Ind. Health* **2019**, *35*, 627−637.

https://doi.org/10.1021/acsomega.1c02981
ACS Omega 2021, 6, 23960−23976

(39) Yousef, M. I.; Mutar, T. F.; Kamel, M. A. E. Hepato-renal toxicity of oral sub-chronic exposure to aluminum oxide and/or zinc oxide nanoparticles in rats. *Toxicol. Rep.* **2019**, *6*, 336−346.
(40) Yang, Y.; Lan, J.; Xu, Z.; Chen, T.; Zhao, T.; Cheng, T.; Zhang, H.; et al. Toxicity and biodistribution of aqueous synthesized ZnS and ZnO quantum dots in mice. *Nanotoxicology* **2014**, *8*, 107−116.
(41) Tang, Y.; Chen, B.; Hong, W.; Chen, L.; Yao, L.; Zhao, Y.; Aguilar, Z. P.; Xu, H. ZnO Nanoparticles Induced Male Reproductive Toxicity Based on the Effects on the Endoplasmic Reticulum Stress Signaling Pathway. *Int. J. Nanomed.* **2019**, *14*, 9563−9576.
(42) Hofmann, A. F.; Hagey, L. R. Bile Acids: Chemistry, Pathochemistry, Biology, Pathobiology and Therapeutics. *Cell. Mol. Life Sci.* **2008**, *65*, 2461−2483.
(43) Botros, M.; Sikaris, K. A. The de ritis ratio: the test of time. *Clin. Biochem. Rev.* **2013**, *34*, 117−130.
(44) Hoffmann, W. E.; Solter, F. *Clinical Biochemistry of Domestic Animals*, 6th ed.; Diagnostic Enzymology of Domestic Animals/ Academic Press, 2008; pp 351−378.
(45) Sizova, E.; Miroshnikov, S.; Nechitailo, X. Assessment of the structural reorganization of liver and biochemical parameters of blood serum after introduction of zinc nanoparticles and its oxides. *Environ. Sci. Pollut. Res. Int.* **2019**, *26*, 17110−17120.
(46) Yao, Y.; Zang, Y.; Qu, J.; Tang, M.; Zhang, T. The Toxicity of Metallic Nanoparticles on Liver: the Subcellular Damages, Mechanisms, and Outcomes. *Int. J. Nanomed.* **2019**, *14*, 8787−8804.
(47) Shalan, H.; Kato, M.; Cheruzel, L. Keeping the spotlight on cytochrome P450. *Biochim. Biophys. Acta, Proteins Proteomics* **2018**, *1866*, 80−87.
(48) Sharma, V.; Anderson, D.; Dhawan, A. Zinc oxide nanoparticles induce oxidative DNA damage and ROS-triggered mitochondria mediated apoptosis in human liver cells (HepG2). *Apoptosis* **2012**, *17*, 852−70.
(49) Veklich, T. O.; Labyntseva, R. D.; Shkrabak, O. A.; Tsymbalyuk, O. V.; Rodik, R. V.; Kalchenko, V. I.; Kosterin, S. O. Inhibition of Na(+), K(+)-ATPase and activation of myosin ATPase by calix[4]arene C-107 cause stimulation of isolated smooth muscle contractile activity. *Ukr. Biochem. J.* **2020**, *92*, 21−30.
(50) Tsymbaliuk, O. V.; Kosterin, S. O. Na^+, K^+-ATPase, endogenous cardiotonic steroids and their transducing role. *Ukr. Biokhim. Zh.* **2012**, *84*, 5−17.
(51) Wu, T.; Tang, M. The inflammatory response to silver and titanium dioxide nanoparticles in the central nervous system. *Nanomedicine* **2018**, *13*, 233−249.
(52) Tsugita, M.; Morimoto, N.; Nakayama, M. SiO_2 and TiO_2 nanoparticles synergistically trigger macrophage inflammatory responses. *Part Fibre Toxicol.* **2017**, *14*, No. 11.
(53) De Matteis, V. Exposure to Inorganic Nanoparticles: Routes of Entry, Immune Response, Biodistribution and In Vitro/In Vivo Toxicity Evaluation. *Toxics* **2017**, *5*, No. 29.
(54) Bettini, S.; Boutet-Robinet, E.; Cartier, C.; Coméra, C.; Gaultier, E.; Dupuy, J.; Naud, N.; Taché, S.; Grysan, P.; Reguer, S.; Thieriet, N.; Réfrégiers, M.; Thiaudière, D.; Cravedi, J. P.; Carrière, M.; Audinot, J. N.; Pierre, F. H.; Guzylack-Piriou, L.; Houdeau, E. Food-grade TiO_2 impairs intestinal and systemic immune homeostasis, initiates preneoplastic lesions and promotes aberrant crypt development in the rat colon. *Sci. Rep.*, **2017**, *7*, No. 40373.
(55) Nogueira, C. M.; de Azevedo, W. M.; Dagli, M. L. Z.; Toma, S. H.; de Arruda Leite, A. Z.; Lordello, M. L.; Nishitokukado, I.; Ortiz-Agostinho, C. L.; Duarte, M. I. S.; Ferreira, M. A.; Sipahi, A. M. Titanium dioxide induced inflammation in the small intestine. *World J. Gastroenterol,* **2012**, *18*, 4729−4735.
(56) Yang, J.; Luo, M.; Tan, Z.; Dai, M.; Xie, M.; Lin, J.; Hua, H.; Ma, Q.; Zhao, J.; Liu, A. Oral administration of nano-titanium dioxide particle disrupts hepatic metabolic functions in a mouse model. *Environ. Toxicol. Pharmacol.* **2017**, *49*, 112−118.
(57) Abbasi-Oshaghi, E.; Mirzaei, F.; Pourjafar, M. NLRP3 inflammasome, oxidative stress, and apoptosis induced in the intestine and liver of rats treated with titanium dioxide nanoparticles: in vivo and in vitro study. *Int. J. Nanomed.* **2019**, *14*, 1919−1936.
(58) Jia, X.; Wang, S.; Zhou, L.; Sun, L. The Potential Liver, Brain, and Embryo Toxicity of Titanium Dioxide Nanoparticles on Mice. *Nanoscale Res Lett.* **2017**, *12*, No. 478.
(59) Aboulhoda, B. E.; Abdeltawab, D. A.; Rashed, L. A.; Abd Alla, M. F.; Yassa, H. D. Hepatotoxic Effect of Oral Zinc Oxide Nanoparticles and the Ameliorating Role of Selenium in Rats: A histological, immunohistochemical and molecular study. *Tissue Cell* **2020**, *67*, No. 101441.
(60) Esmaeillou, M.; Moharamnejad, M.; Hsankhani, R.; Tehrani, A. A.; Maadi, H. Toxicity of ZnO nanoparticles in healthy adult mice. *Environ. Toxicol. Pharmacol,* **2013**, *35*, 67−71.
(61) Kong, T.; Zhang, S. H.; Zhang, C.; Zhang, J. L.; Yang, F.; Wang, G. Y.; Yang, Z. J.; Bai, D. Y.; Zhang, M. Y.; Wang, J.; Zhang, B. H. Long-Term Effects of Unmodified 50 nm ZnO in Mice. *Biol. Trace Elem. Res.* **2019**, *189*, 478−489.
(62) Fricker, G.; Fahr, A. Mechanisms of hepatic transport of cyclosporin A: an explanation for its cholestatic action. *Yale J. Biol. Med.* **1997**, *70*, 379−390.
(63) Garduño-Siciliano, L.; Labarrios, F.; Tamariz, J.; Moreno, M. G.; Chamorro, G.; Muriel, P. Effect of alpha-asarone and a derivative on lipids, bile flow and Na^+/K^+-ATPase in ethinyl estradiol-induced cholestasis in the rat. *Fundam Clin Pharmacol.* **2007**, *21*, 81−88.
(64) Proceedings of the 39th plenary meeting. Scientific committee on toxicity, ecotoxicity and the environment opinion on the results of the risk assessment of: Zinc metal (CAS No. 7440-66-6), Zinc chloride (CAS No. 7646-85-7), Zinc sulphate (CAS No. 7733-02-0), Zinc distearate (CAS No. 557-05-1, 9105-01-3), Zinc phosphate (CAS No. 779-90-0), Zinc oxide (CAS No. 1314-13-2) Human Health Part, Belgian, Brussels , 2003.
(65) Wang, Y.; Chen, Z.; Ba, T.; Pu, J.; Chen, T.; Song, Y.; Gu, Y.; Qian, Q.; Xu, Y.; Xiang, K.; Wang, H.; Jia, G. Susceptibility of young and adult rats to the oral toxicity of titanium dioxide nanoparticles. *Small* **2013**, *9*, 1742−1752.
(66) Nasibyan, L. S.; Filippov, I. B. Modulation of rat myometrium contractions via *Staphylococcus aureus* cell wall peptidoglycan. *Physiol. J.* **2014**, *60*, 62−72.
(67) Reitman, S.; Frankel, S. A colorimetric method for determination of serum glutamate oxaloacetate and glutamic pyruvate transaminase. *Am. J. Clin. Pathol.* **1957**, *28*, 56−58.
(68) Jendrassik, L.; Grof, P. Colorimetric Method of Determination of Bilirubin. *Biochem. Z.* **1939**, *297*, 81−82.
(69) Cohen, P. P.; Thompson, F. L. Mechanism of the thymol turbidity test. *J. Lab. Clin. Med.* **1947**, *32*, 475−480.
(70) Veselsky, S. P.; Lyashchenko, P. S.; Lukyanenko, I. A. Auth. certificate No. 441106614 USSR MTIS 01W33 / 50. A method for determining bile acids in biological fluids. USSR No.1624322 declared 25.01.1988, published 30.01.1991.
(71) Lowry, O. H.; Rosebrough, N. J.; Farr, A. L.; Randall, R. J. Protein measurement with the Folin phenol reagent. *J. Biol. Chem.* **1951**, *193*, 265−275.
(72) Tsymbalyuk, O. V.; Kosterin, S. O.; Rodik, R. V.; Kalchenko, V. I. Comparative study in vitro and in vivo of the effects of calixarene C107 and oubaine on Na^+, K^+-ATPase activity in the plasma membranes of rat hepatocytes. *J. Ukr. Biochem.* **2010**, *82*, 78−85.
(73) Rathbun, W. B.; Betlach, M. V. Estimation of enzymically produced orthophosphate in the presence of cysteine and adenosine triphosphate. *Anal. Biochem.* **1969**, *28*, 436−445.

https://doi.org/10.1021/acsomega.1c02981
ACS Omega 2021, 6, 23960−23976